Supplementary Information for

Thermoresponsive Lactate Amide Acrylic Polymers Developed from PLA Bags

Marc Palà,[†] Alina Ismagilova,[Δ] Adrian Moreno,[†] Jorge Plaza,[†] Juan C. Ronda,[†] Marina Galià,[†] Lauri Vares,[Δ] Gerard Lligadas[,†]*

[†] University Rovira i Virgili, Laboratory of Sustainable Polymers, Department of Analytical Chemistry and Organic Chemistry, C/ Marcel·lí Domingo 1, 43007 Tarragona, Spain.

[Δ] Institute of Technology, University of Tartu, Nooruse 1, Tartu 50411, Estonia

This supporting information contains:

- Total number of pages: 36
- Total number of figures: 38
- Total number of tables: 3

Characterization of LA derivatives

(*S*)-2-hydroxypropanamide (LA1) was obtained (yield = 98%) as a colorless oil. ^{1}H NMR (401 MHz, $CDCl_3$) δ 4.23 (q, *J* = 6.9 Hz, 1H), 1.36 (d, *J* = 7.0 Hz, 3H). ^{13}C NMR (101 MHz, $CDCl_3$) δ 180.82, 67.40, 19.56.

(*S*)-*N*-ethyl-2-hydroxypropanamide (LA2) was obtained (yield = 45%) as a yellowish oil. ^{1}H NMR (401 MHz, $CDCl_3$) δ 6.44 (bs, 1H), 4.27 – 4.17 (m, 1H), 3.32 (qd, *J* = 7.3, 5.7 Hz, 2H), 2.60 (s, 1H), 1.43 (d, *J* = 6.8 Hz, 3H), 1.17 (t, *J* = 7.3 Hz, 3H). ^{13}C NMR (101 MHz, $CDCl_3$) δ 174.49, 68.50, 34.14, 21.45, 14.90.

(*S*)-2-hydroxy-*N*-propylpropanamide (LA3) was obtained (yield = 80%) as a yellowish oil. ^{1}H NMR (401 MHz, CDCl3) δ 6.75 (bs, 1H), 4.19 (q, *J* = 6.8 Hz, 1H), 3.62 (bs, 1H), 3.27–3.14 (m, 2H), 1.48–1.58 (m, 2H), 1.40 (d, *J* = 6.8 Hz, 3H), 0.91 (t, *J* = 7.4 Hz, 3H). ^{13}C NMR (101 MHz, CDCl3) δ 174.84, 68.33, 40.78, 22.77, 21.29, 11.29.

(*S*)-2-hydroxy-*N*-isopropylpropanamide (LA4) was obtained (yield = 70%) as a yellowish oil. ^{1}H NMR (401 MHz, CDCl3) δ 6.52 (bs, 1H), 4.15 (q, *J* = 6.8 Hz, 1H), 4.03 (dp, *J* = 8.2, 6.6 Hz, 1H), 3.67 (bs, 1H), 1.39 (d, *J* = 6.8 Hz, 3H), 1.15 (d, *J* = 6.6 Hz, 6H). ^{13}C NMR (101 MHz, CDCl3) δ 174.01, 68.36, 41.15, 22.79, 21.37.

(*S*)-2-hydroxy-*N*-(2-methoxyethyl)propenamide (LA5) was obtained as a yellowish oil. ^{1}H NMR (401 MHz, CDCl3) δ 7.11 (bs, 1H), 4.18 (q, *J* = 6.9 Hz, 1H), 3.50–3.36 (m, 4H), 3.33 (s, 3H), 1.38 (d, *J* = 6.9 Hz, 3H). ^{13}C NMR (101 MHz, CDCl3) δ 175.07, 71.20, 68.29, 58.82, 38.37, 20.78.

(*S*)-*N*,*N*-diethyl-2-hydroxypropanamide (LA6) was obtained (yield = 82%) as a yellowish oil. ^{1}H NMR (401 MHz, $CDCl_3$) δ 4.37 (dq, *J* = 7.7, 6.5 Hz, 1H), 3.82 (d, *J* = 7.6 Hz, 1H), 3.50 (dq, *J* = 14.1, 7.1 Hz, 1H), 3.36–3.13 (m, 3H), 1.30 (d, *J* = 6.5 Hz, 3H), 1.19 (t, *J* = 7.2 Hz, 3H), 1.12 (t, *J* = 7.2 Hz, 3H). ^{13}C NMR (101 MHz, $CDCl_3$) δ 174.43, 64.28, 40.94, 40.30, 21.91, 14.20, 12.88.

(2*S*)-2-hydroxy-*N*-((tetrahydrofuran-2-yl)methyl)propenamide (LA7) was obtained (yield = 94%) as a yellowish oil.^{1}H NMR (401 MHz, $CDCl_3$) δ 6.79 (bs, 1H), 4.24 (qd, J = 6.8, 1.7 Hz, 1H), 3.98 (dddd, *J* = 10.1, 7.2, 5.2, 2.8 Hz, 1H), 3.87 (dt, *J* = 8.3, 6.6 Hz, 1H), 3.76 (dtd, *J* = 8.3, 6.8, 1.4 Hz, 1H), 3.59 (dddd, *J* = 13.8, 6.6, 4.7, 3.3 Hz, 1H), 3.18 (dtd, *J* = 13.9, 7.3, 5.1 Hz, 1H), 2.84 (s, 1H), 2.09–1.79 (m, 3H), 1.61–1.48 (m, 1H), 1.44 (dd, *J* = 6.8, 1.1 Hz, 3H). ^{13}C NMR (101 MHz, $CDCl_3$) δ 174.71, 77.84, 68.36, 68.16, 42.87, 28.64, 25.84, 21.34.

(*S*)-2-hydroxy-1-(pyrrolidin-1-yl)propan-1-one (LA8) was obtained (yield = 91%) as a yellowish oil. ^{1}H NMR (401 MHz, $CDCl_3$) δ 4.24 (q, *J* = 6.6 Hz, 1H), 3.75 (bs, 1H), 3.51 (dt, *J* = 12.0, 7.4 Hz, 1H), 3.46–3.36 (m, 2H), 3.28 (dt, *J* = 10.2, 6.9 Hz, 1H), 2.02–1.74 (m, 4H), 1.28 (d, J = 6.6 Hz, 3H). ^{13}C NMR (101 MHz, $CDCl_3$) δ 173.51, 65.53, 46.26, 45.97, 26.08, 23.91, 20.63.

(*S*)-2-hydroxy-1-morpholinopropan-1-one (LA9) was obtained (yield = 70%) as a yellowish oil. ^{1}H NMR (401 MHz, CDCl3) δ 4.44 (p, J = 6.8 Hz, 1H), 3.79–3.59 (m, 7H), 3.45–3.39 (m, 2H), 1.33 (d, J = 6.6 Hz, 3H). ^{13}C NMR (101 MHz, CDCl3) δ 173.87, 66.89, 66.47, 64.13, 45.49, 42.87, 21.47.

Characterization of LAA monomers

(*S*)-1-(dimethylamino)-1-oxopropan-2-yl acrylate (LAA0) was obtained (yield = 73%) as a colorless oil. $[\alpha]_D^{20} = -6.320$ deg·dm^{-1}·cm^3·g^{-1} (52.8 mg·mL^{-1}, MeCN). ^{1}H NMR (401 MHz, $CDCl_3$) δ 6.46 (dd, *J* = 17.4, 1.4 Hz, 1H), 6.18 (dd, *J* = 17.3, 10.4 Hz, 1H), 5.87 (dd, *J* = 10.4, 1.4 Hz, 1H), 5.47 (q, *J* = 6.7 Hz, 1H), 3.07 (s, 3H), 2.97 (s, 3H), 1.47 (d, *J* = 6.8 Hz, 3H). ^{13}C NMR (101 MHz, $CDCl_3$) δ 170.06, 165.65, 131.69, 127.81, 67.00, 36.77, 35.92, 16.63. HRMS (HESI-Orbitrap) calculated for $[M + Na]^+$ $C_8H_{13}NNaO_3^+$ (*m/z*): 194.0787; found: 194.0789.

(*S*)-1-amino-1-oxopropan-2-yl acrylate (LAA1) was obtained (yield = 62%) as a yellowish oil after purification by column chromatography (AcOEt : Hx, 2:1). $[\alpha]_D^{20} = -5.295$ deg·dm^{-1}·cm^3·g^{-1} (50.0 mg·mL^{-1}, MeCN). ^{1}H NMR (401 MHz, $CDCl_3$) δ 6.64 (s, 1H), 6.42 (dd, *J* = 17.3, 1.3 Hz, 1H), 6.30 (s, 1H), 6.12 (dd, *J* = 17.3, 10.4 Hz, 1H), 5.86 (dd, *J* = 10.4, 1.3 Hz, 1H), 5.19 (q, *J* = 6.9 Hz, 1H), 1.45 (d, *J* = 6.9 Hz, 3H). ^{13}C NMR (101 MHz, $CDCl_3$) δ 173.75, 164.86, 132.36, 127.65, 70.32, 17.75. HRMS (HESI-Orbitrap) calculated for $[M + Na]^+$ $C_6H_9NO_3Na^+$ (*m/z*): 166.0492, found, 166.0475.

(*S*)-1-(ethylamino)-1-oxopropan-2-yl acrylate (LAA2) was obtained (yield = 47%) as a white solid after purification by column chromatography (AcOEt : Hx, 2:1). $[\alpha]_D^{20} = -18.169$ deg·dm^{-1}·cm^3·g^{-1} (11.2 mg·mL^{-1}, MeCN). ^{1}H NMR (401 MHz, $CDCl_3$) δ 6.49 (dd, *J* = 17.3, 1.3 Hz, 1H), 6.18 (dd, *J* = 17.3, 10.4 Hz, 1H), 6.10 (bs, 1H), 5.93 (dd, *J* = 10.4, 1.3 Hz, 1H), 5.29 (q, *J* = 6.8 Hz, 1H), 3.32 (q, *J* = 7.3 Hz, 2H), 1.50 (d, *J* = 6.9 Hz, 3H), 1.15 (t, *J* = 7.3 Hz, 3H). ^{13}C NMR (101 MHz, $CDCl_3$) δ 170.21, 164.77, 132.32, 127.85, 70.86, 34.30, 17.99, 14.88. HRMS (HESI-Orbitrap) calculated for $[M + Na]^+$ $C_8H_{13}NO_3Na^+$ (*m/z*): 194.0786; found: 194.0785.

(*S*)-1-oxo-1-(propylamino)propan-2-yl acrylate (LAA3) was obtained (yield = 63%) as a white solid. $[\alpha]_D^{20}$ = −21.813 deg·dm^{-1}·cm^3·g^{-1} (53.1 mg·mL^{-1}, MeCN). ^{1}H NMR (401 MHz, $CDCl_3$) δ 6.47 (dd, *J* = 17.3, 1.3 Hz, 1H), 6.17 (dd + bs, *J* = 17.3, 10.4 Hz, 2H), 5.91 (dd, *J* = 10.4, 1.3 Hz, 1H), 5.26 (q, *J* = 6.9 Hz, 1H), 3.22 (q, *J* = 6.0 Hz, 2H), 1.57–1.47 (m, 5H), 0.90 (t, *J* = 7.4 Hz, 3H). ^{13}C NMR (101 MHz, $CDCl_3$) δ 170.27, 164.76, 132.29, 127.80, 70.86, 40.97, 22.85, 18.01, 11.33. HRMS (HESI-Orbitrap) calculated for $[M + Na]^+$ $C_9H_{15}NO_3Na^+$ (*m/z*): 208.0944; found: 208.0942.

(*S*)-1-(isopropylamino)-1-oxopropan-2-yl acrylate (LAA4) was obtained (yield = 62%) as a white solid. $[\alpha]_D^{20}$ = −16.042 deg·dm^{-1}·cm^3·g^{-1} (49.9 mg·mL^{-1}, MeCN). ^{1}H NMR (401 MHz, $CDCl_3$) δ 6.49 (dd, *J* = 17.3, 1.3 Hz, 1H), 6.19 (dd, *J* = 17.3, 10.4 Hz, 1H), 5.93 (dd, *J* = 10.5, 1.3 Hz, 1H), 5.85 (bs, 1H), 5.25 (q, *J* = 6.8 Hz, 1H), 4.09 (dp, *J* = 8.0, 6.5 Hz, 1H), 1.50 (d, *J* = 6.8 Hz, 3H), 1.17 (dd, *J* = 8.4, 6.6 Hz, 6H). ^{13}C NMR (101 MHz, $CDCl_3$) δ 169.42, 164.78, 132.26, 127.89, 70.88, 41.38, 22.78, 17.97. HRMS (HESI-Orbitrap) calculated for $[M + Na]^+$ $C_9H_{15}NO_3Na^+$ (*m/z*): 208.0944; found: 208.0941.

(*S*)-1-((2-methoxyethyl)amino)-1-oxopropan-2-yl acrylate (LAA5) was obtained (yield = 63%) as a white solid. $[\alpha]_D^{20}$ = −14.981 deg·dm^{-1}·cm^3·g^{-1} (51.1 mg·mL^{-1}, MeCN). ^{1}H NMR (401 MHz, $CDCl_3$) δ 6.49 (dd + bs, *J* = 17.3, 1.3 Hz, 2H), 6.19 (dd, *J* = 17.3, 10.4 Hz, 1H), 5.93 (dd, *J* = 10.4, 1.3 Hz, 1H), 5.30 (q, *J* = 6.8 Hz, 1H), 3.51–3.43 (m, 4H), 3.36 (s, 3H), 1.52 (d, *J* = 6.8 Hz, 3H). ^{13}C NMR (101 MHz, $CDCl_3$) δ 170.48, 164.75, 132.22, 127.89, 71.12, 70.86, 58.96, 39.08, 18.01. HRMS (HESI-Orbitrap) calculated for $[M + Na]^+$ $C_9H_{15}NO_4Na^+$ (*m/z*): 224.0893; found: 224.0888.

(*S*)-1-(diethylamino)-1-oxopropan-2-yl acrylate (LAA6) was obtained (yield = 47%) as a white solid. $[\alpha]_D^{20}$ = −1.577 deg·dm^{-1}·cm^3·g^{-1} (9.7 mg·mL^{-1}, MeCN). ^{1}H NMR (401 MHz, $CDCl_3$) δ 6.44 (dd, *J* = 17.3, 1.4 Hz, 1H), 6.17 (dd, *J* = 17.3, 10.4 Hz, 1H), 5.85 (dd, *J* = 10.4, 1.4 Hz, 1H), 5.40 (q, *J* = 6.7 Hz, 1H), 3.53 – 3.21 (m, 4H), 1.46 (d, *J* = 6.7 Hz, 3H), 1.24 (t, *J* = 7.2 Hz, 3H), 1.11 (t, *J* = 7.1 Hz, 3H). ^{13}C NMR (101 MHz, $CDCl_3$) δ 169.42, 165.80, 131.65, 128.06, 67.23, 41.74, 40.69, 17.39, 14.36, 12.93. HRMS (HESI-Orbitrap) calculated for $[M + Na]^+$ $C_{10}H_{17}NO_3Na^+$ (*m/z*): 222.1101; found: 222.1095.

(2*S*)-1-oxo-1-(((tetrahydrofuran-2-yl)methyl)amino)propan-2-yl acrylate (LAA7) was obtained (yield = 66%) as a colorless oil. $[\alpha]_D^{20}$ = −16.74 deg·dm^{-1}·cm^3·g^{-1} (54.7 mg·mL^{-1}, MeCN). ^{1}H NMR (401 MHz, $CDCl_3$) δ 6.52–6.40 (d + bs, 2H), 6.18 (ddd, *J* = 17.3, 10.4, 1.7

Hz, 1H), 5.92 (ddd, *J* = 10.5, 2.6, 1.3 Hz, 1H), 5.29 (qd, *J* = 6.8, 3.1 Hz, 1H), 4.01–3.91 (m, 1H), 3.89–3.70 (m, 2H), 3.60–3.51 (m, 1H), 3.28–3.16 (m, 1H), 2.03–1.82 (m, 3H), 1.58–1.45 (m, 4H). ^{13}C NMR (101 MHz, $CDCl_3$) δ 170.5, 164.8, 132.3, 127.9, 77.7, 70.9, 68.37, 42.92, 42.73, 28.62, 26.06, 18.09. HRMS (HESI-Orbitrap) calculated for $[M + Na]^+$ $C_{11}H_{17}NO_4Na^+$ (*m/z*): 250.1050; found: 250.1048.

(*S*)-1-oxo-1-(pyrrolidin-1-yl)propan-2-yl acrylate (LAA8*)* was obtained (yield = 58%) as a white solid. $[\alpha]_D^{20} = -2.767$ deg·dm^{-1}·cm^3·g^{-1} (52.5 mg·mL^{-1}, MeCN) ^{1}H NMR (401 MHz, $CDCl_3$) δ 6.45 (dd, *J* = 17.3, 1.4 Hz, 1H), 6.18 (dd, *J* = 17.3, 10.4 Hz, 1H), 5.86 (dd, *J* = 10.4, 1.4 Hz, 1H), 5.29 (q, *J* = 6.7 Hz, 1H), 3.70–3.62 (m, 1H), 3.55 (dt, *J* = 11.9, 7.0 Hz, 1H), 3.48–3.34 (m, 2H), 2.04–1.92 (m, 2H), 1.91–1.79 (m, 2H), 1.47 (d, *J* = 6.7 Hz, 3H). ^{13}C NMR (101 MHz, $CDCl_3$) δ 168.71, 165.86, 131.77, 127.98, 68.63, 46.24, 26.33, 24.10, 16.68. HRMS (HESI-Orbitrap) calculated for $[M + Na]^+$ $C_{10}H_{15}NO_3Na^+$ (*m/z*): 220.0944; found: 220.0939.

(*S*)-1-morpholino-1-oxopropan-2-yl acrylate (LAA9) was obtained (yield = 54%) as a colorless oil. $[\alpha]_D^{20} = -3.281$ deg·dm^{-1}·cm^3·g^{-1} (47.8 mg·mL^{-1}, MeCN) ^{1}H NMR (401 MHz, $CDCl_3$) δ 6.47 (dd, *J* = 17.3, 1.3 Hz, 1H), 6.18 (dd, *J* = 17.3, 10.5 Hz, 1H), 5.89 (dd, *J* = 10.4, 1.3 Hz, 1H), 5.46 (q, *J* = 6.8 Hz, 1H), 3.79–3.40 (m, 8H), 1.48 (d, *J* = 6.8 Hz, 3H). ^{13}C NMR (101 MHz, $CDCl_3$) δ 168.82, 165.67, 132.11, 127.80, 67.00, 66.88, 66.66, 46.11, 42.66, 17.01. HRMS (HESI-Orbitrap) calculated for $[M + Na]^+$ $C_{10}H_{15}NO_4Na^+$ (*m/z*): 236.0893; found: 236.0888.

Ecotoxicity studies

Water-TOXTM STD: luminescence inhibition test with bacteria *Aliivibrio fischeri*

The luminescence intensity was measured in GloMax® 20/20 Luminometer. The results were evaluated according to ISO 11348-3 as follows:

1. $KF = \frac{IC_t}{IC_0}$
2. $INH\% = 100 - 100\left[\frac{IT_f}{(KF \times IT_0)}\right]$

Where:

KF – Correction factor

IC_t – Luminescence intensity of negative control after contact time

IC_0 – Initial luminescence intensity of control sample

$INH\%$ – Inhibition percentage of luminescence

IT_t – Luminescence intensity of test sample after contact time

IT_0 – Initial luminescence intensity of test sample

DuckWeed Toxkit F: Growth inhibition test with *Spirodela polyrhiza*

72 h EC_{50} is the concentration of tested substances that will affect 50% of the vegetative buds in the test population after 3 days of exposure to samples.

Percent inhibition of growth rate (I_r) were calculated for each test concentration according to the following formula:

$$I_r = \frac{\mu C - \mu T}{\mu C} \times 100\%$$

Where:

I_r – percent inhibition in average specific growth rate

μ – the size of the vegetative buds measured by Image Analysis software

μC – mean value for μ in the control

μT – mean value for μ in the treatment group

Thamnotoxkit F: Crustacean toxicity screening test with *Thamnocephalus platyurus*

To estimate the amount of alive and dead crustaceans used dissection microscope. Percent mortality were calculated for each test concentration according to the following formula:

$$\%_{mortality} = \frac{N_d}{N_t} \times 100\%$$

Where:

N_d – total number of dead crustaceans

N_t – total number of tested crustaceans

Additional experimental details

Figure S1. Digital image of PLA bags used as starting material.

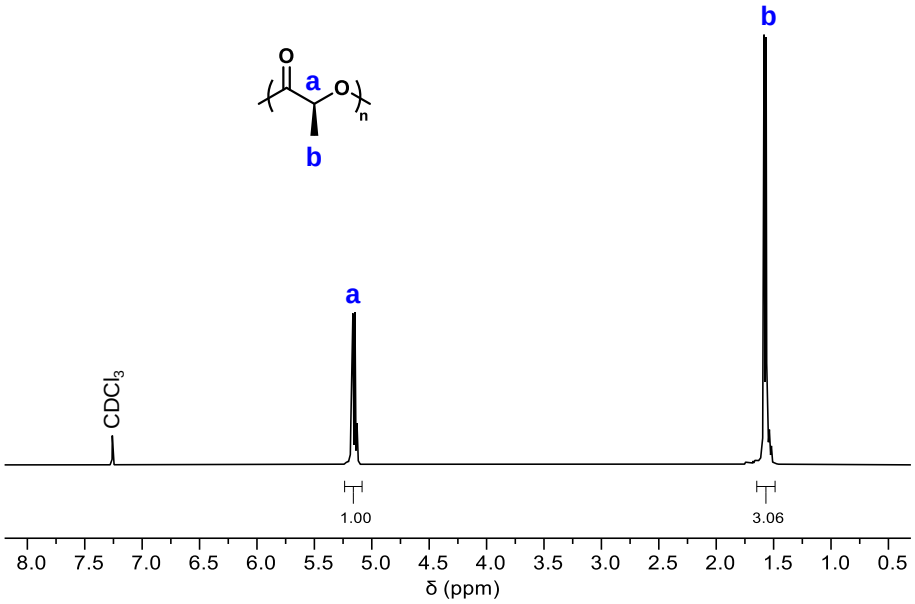

Figure S2. ^{1}H NMR of commercially available PLA bags in $CDCl_3$.

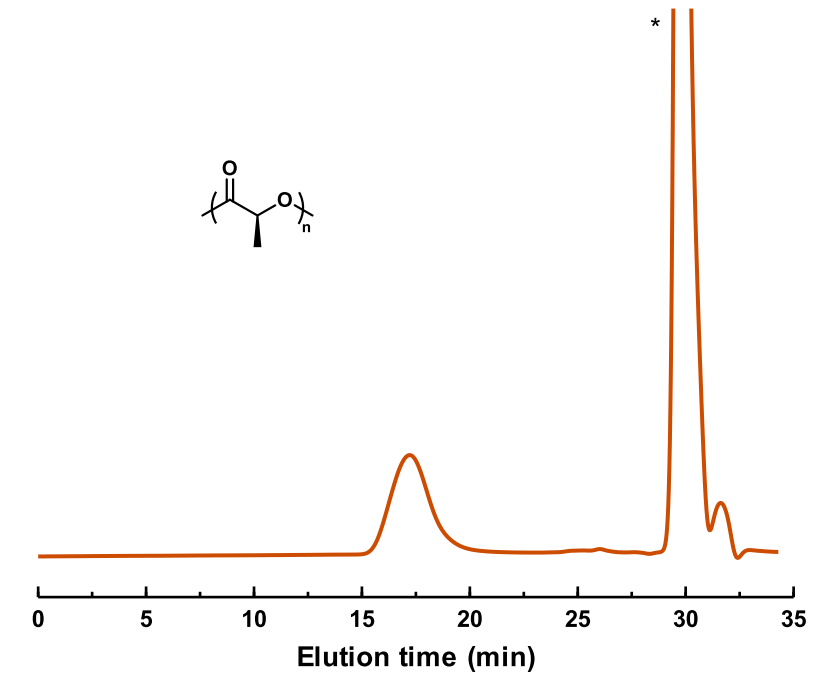

Figure S3. SEC analysis of commercially available PLA bags (M_n^{SEC} = 74,700 g·mol^{-1}, $Đ$ = 1.44). * Corresponds to the peak of the internal standard (toluene).

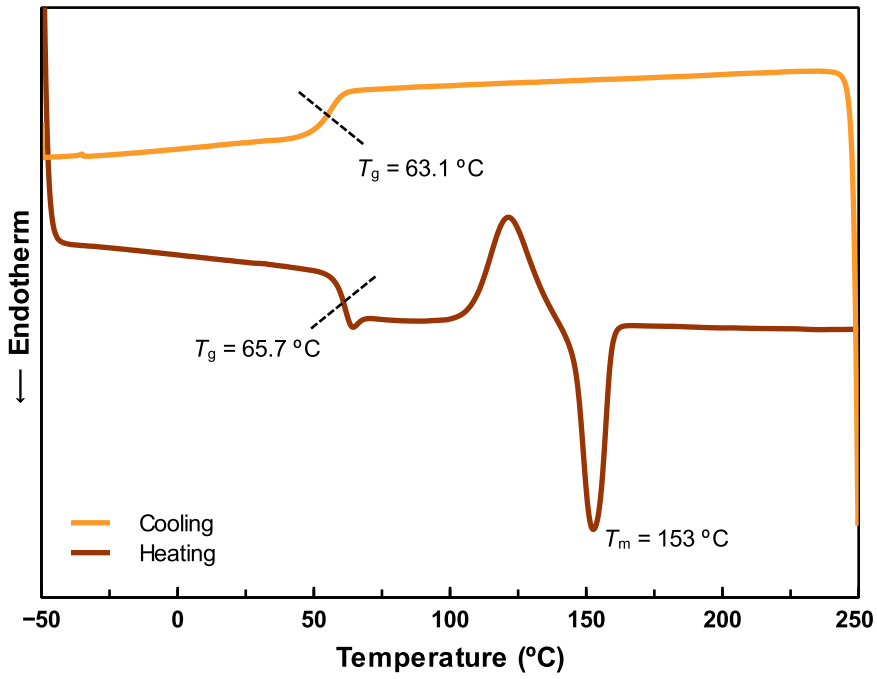

Figure S4. DSC analysis of commercially available PLA bags. Orange trace corresponds to the cooling cycle, while brown graph corresponds to the second heating cycle.

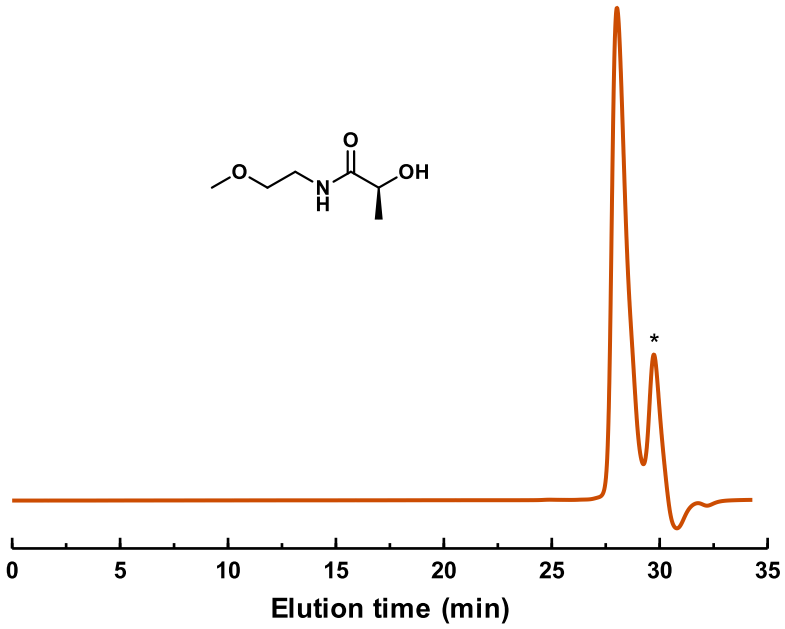

Figure S5. SEC analysis after aminolysis of commercially available PLA bags employing A5 as nucleophile in the presence of TBD to obtain LA5. * Corresponds to the peak of the internal standard (toluene).

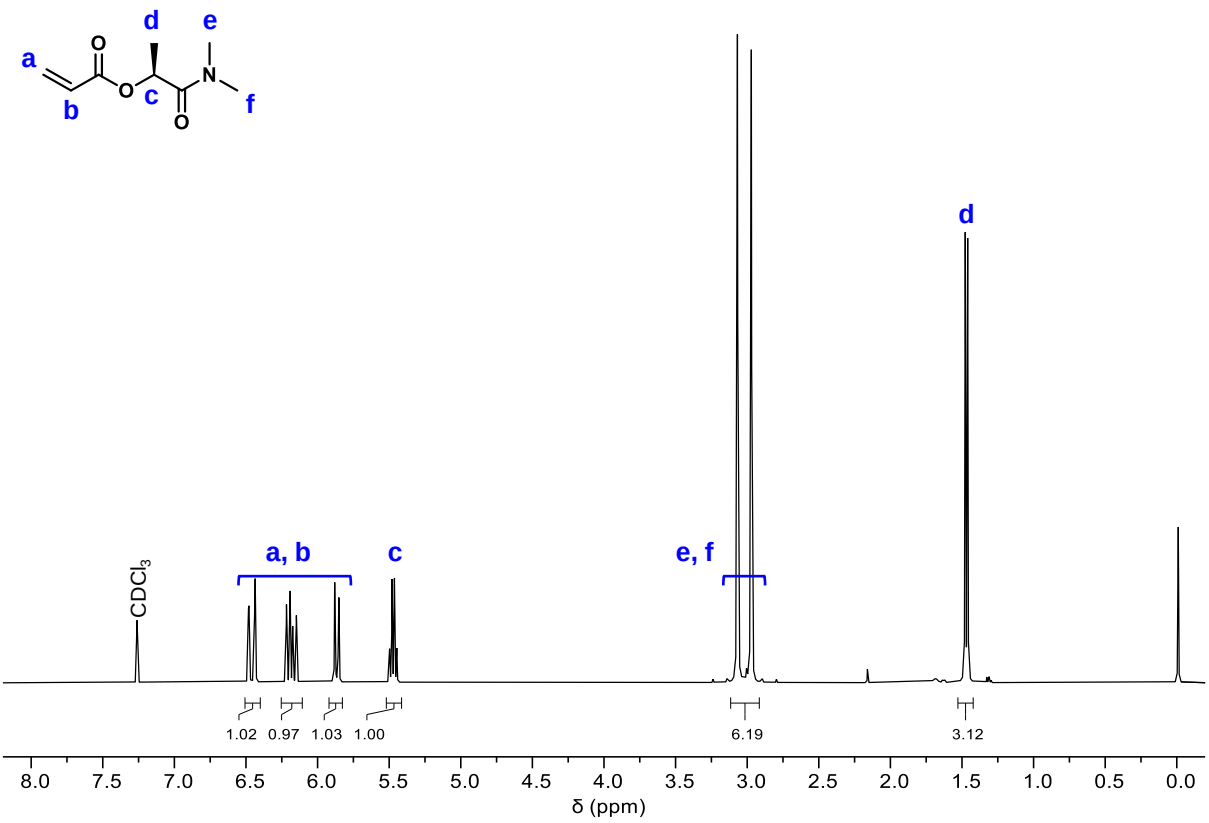

Figure S6. [1]H NMR analysis after aminolysis of commercially available PLA bags employing A5 as nucleophile in the presence of TBD to obtain LA5. After 2 h of reaction at 75 ºC, the spectrum shows the complete vanishment of the signals corresponding to PLA (compare Figure S2) and the characteristic signals of LA5. * Corresponds to the signals of catalyst (TBD) and ** corresponds to the signals of remaining dichloromethane from reaction crude mixture.

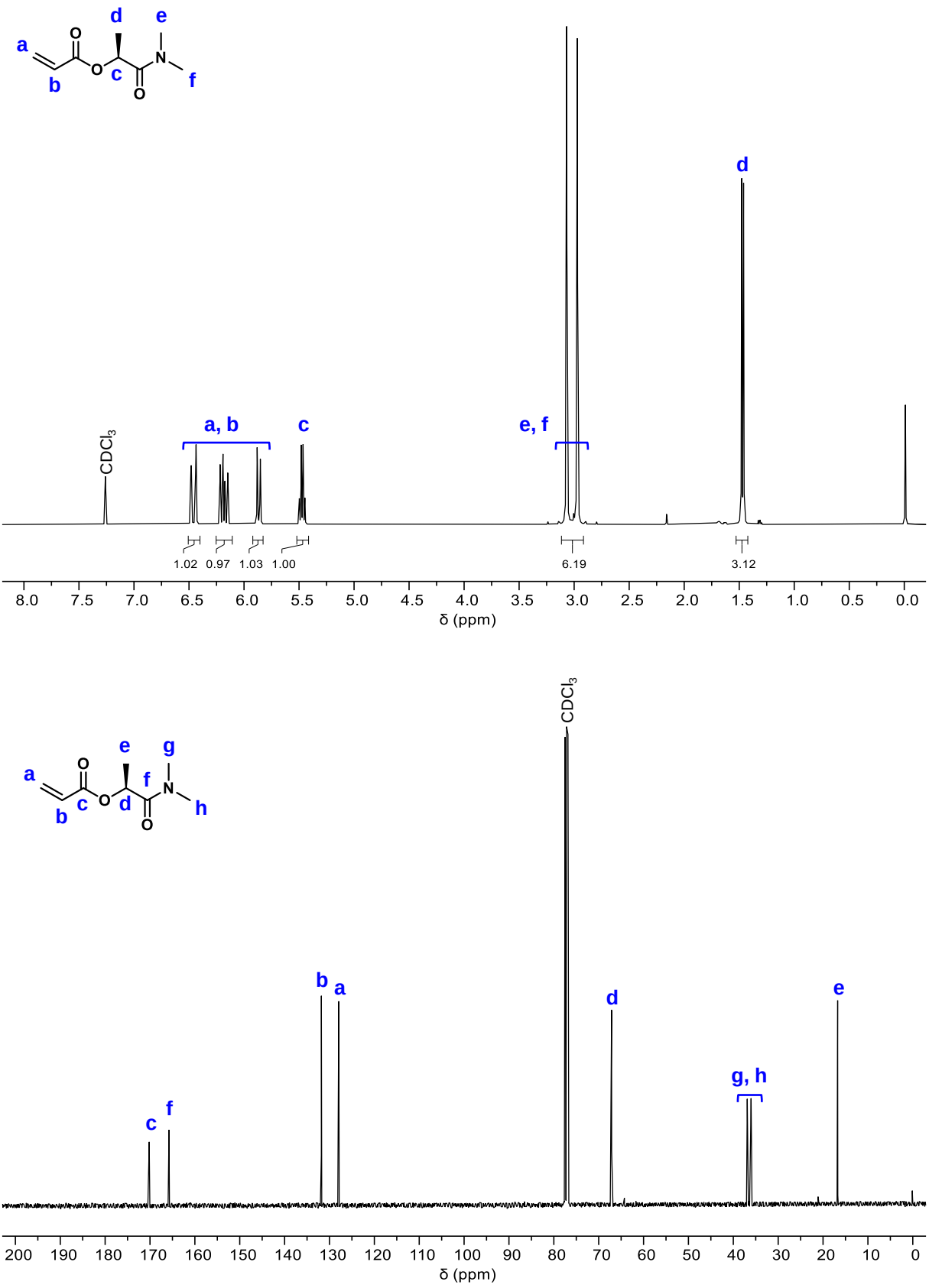

Figure S7. ^{1}H (top) and ^{13}C (bottom) NMR spectra of LAA0 in $CDCl_3$.

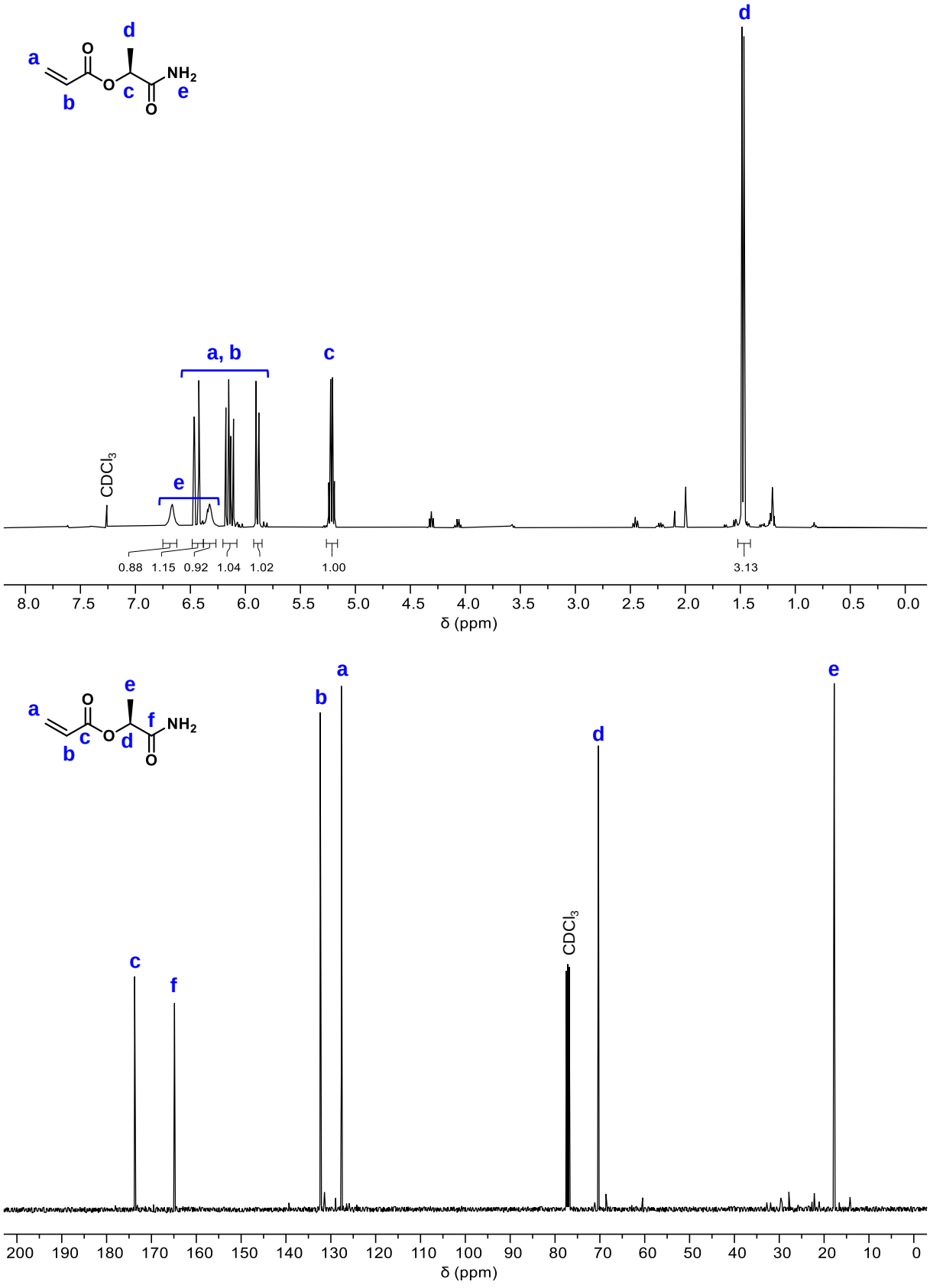

Figure S8. ^{1}H (top) and ^{13}C (bottom) NMR spectra of LAA1 in $CDCl_3$.

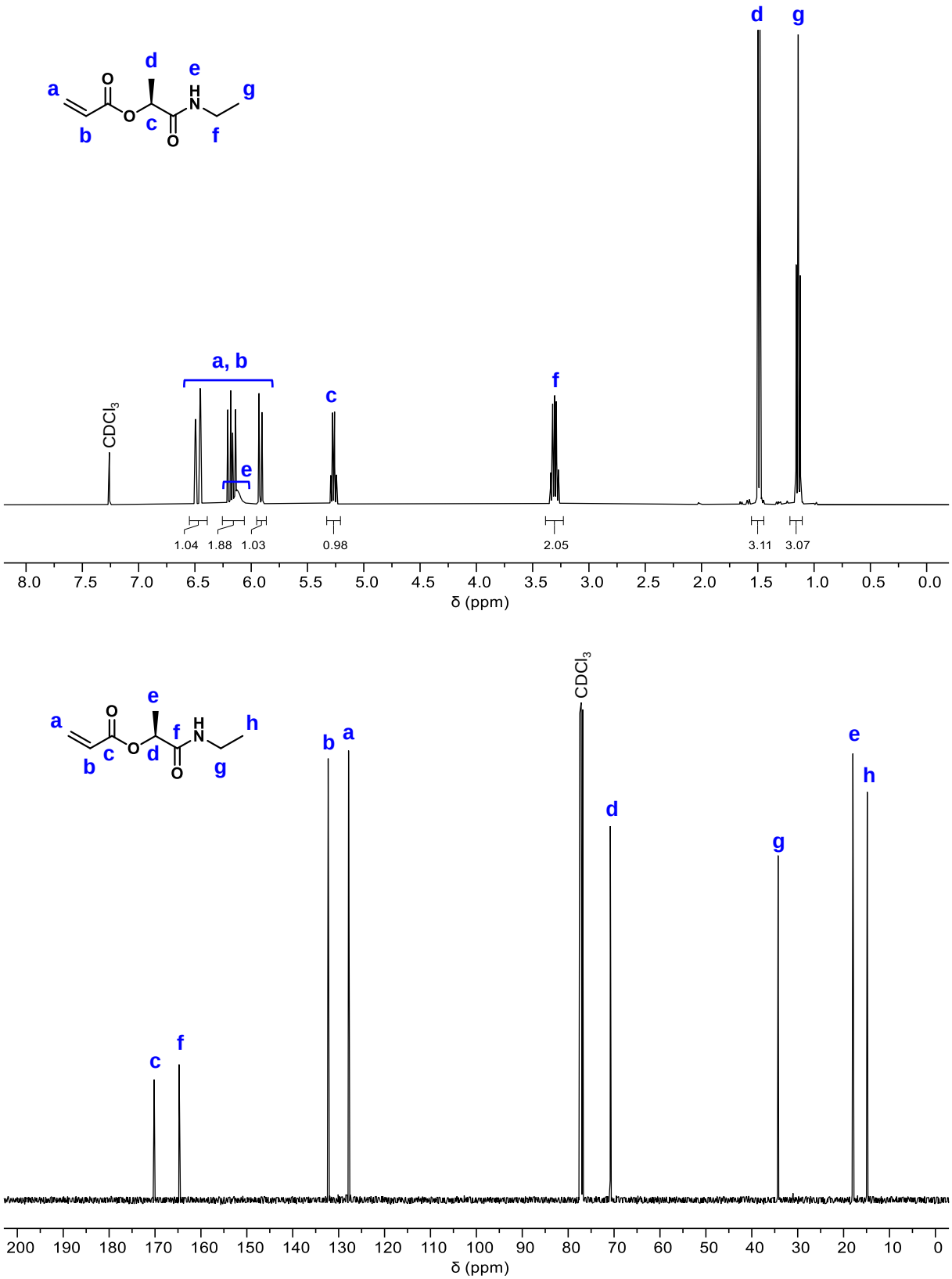

Figure S9. ^{1}H (top) and ^{13}C (bottom) NMR spectra of LAA2 in $CDCl_3$.

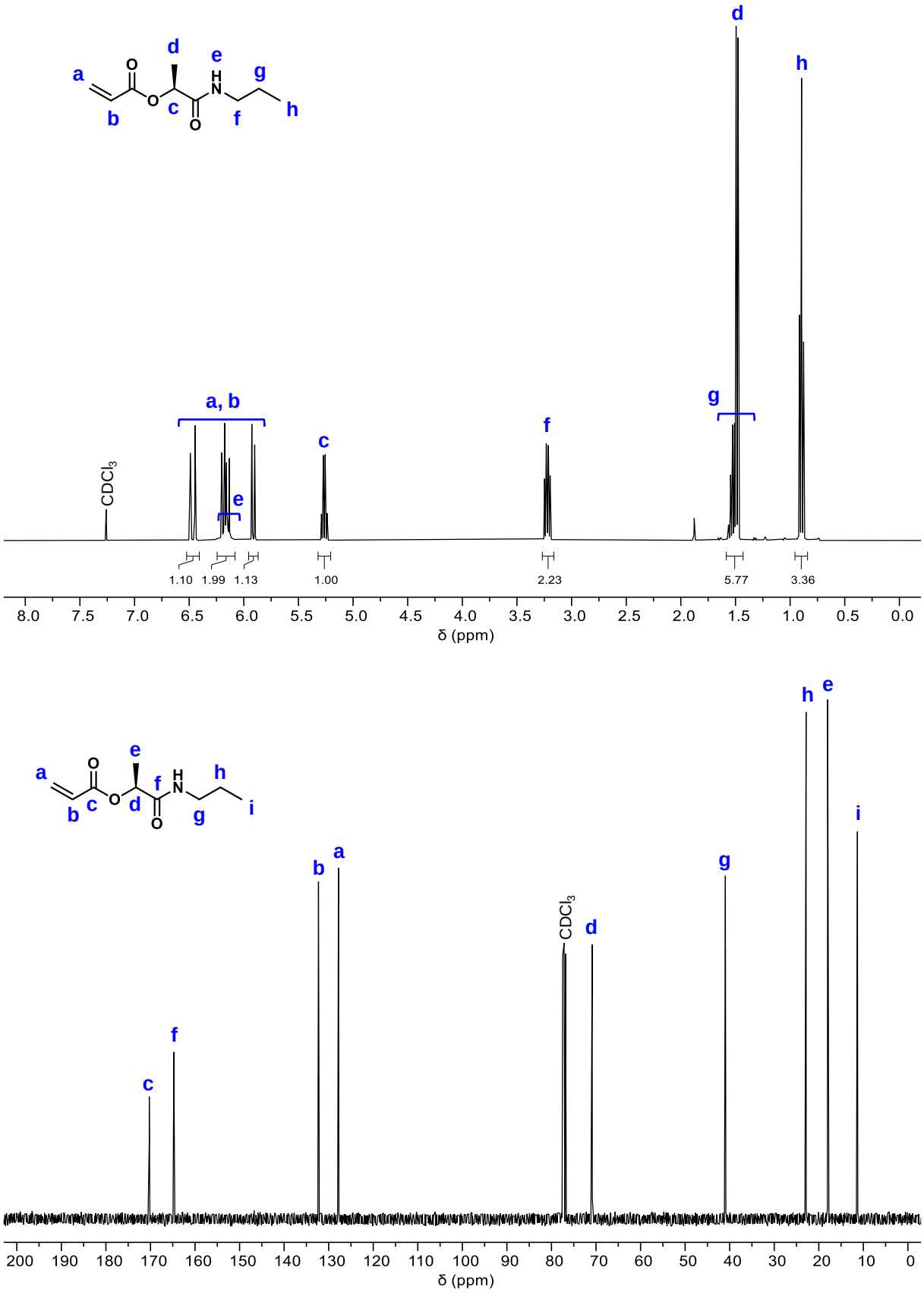

Figure S10. ^{1}H (top) and ^{13}C (bottom) NMR spectra of LAA3 in $CDCl_3$.

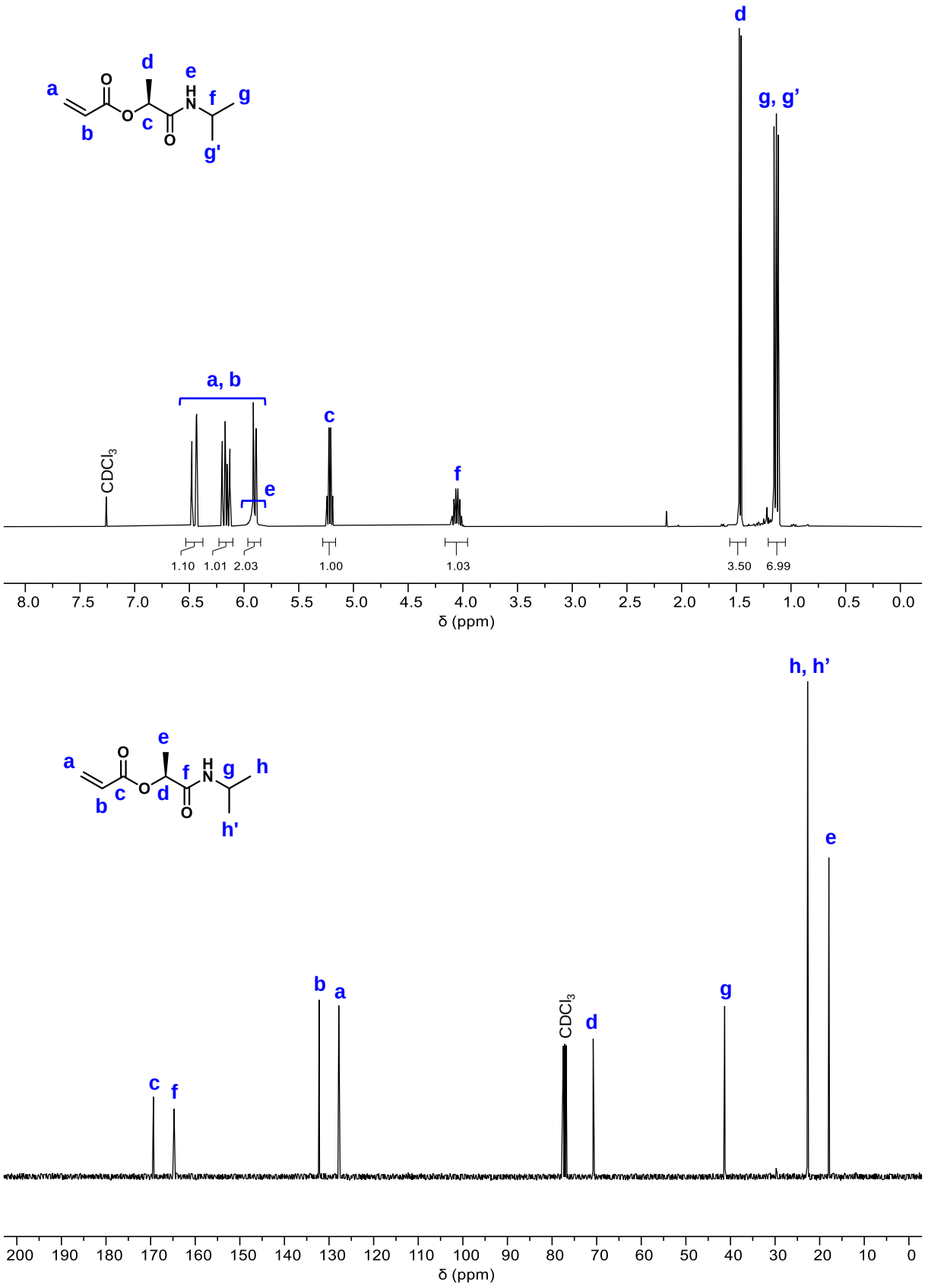

Figure S11. ^{1}H (top) and ^{13}C (bottom) NMR spectra of LAA4 in $CDCl_3$.

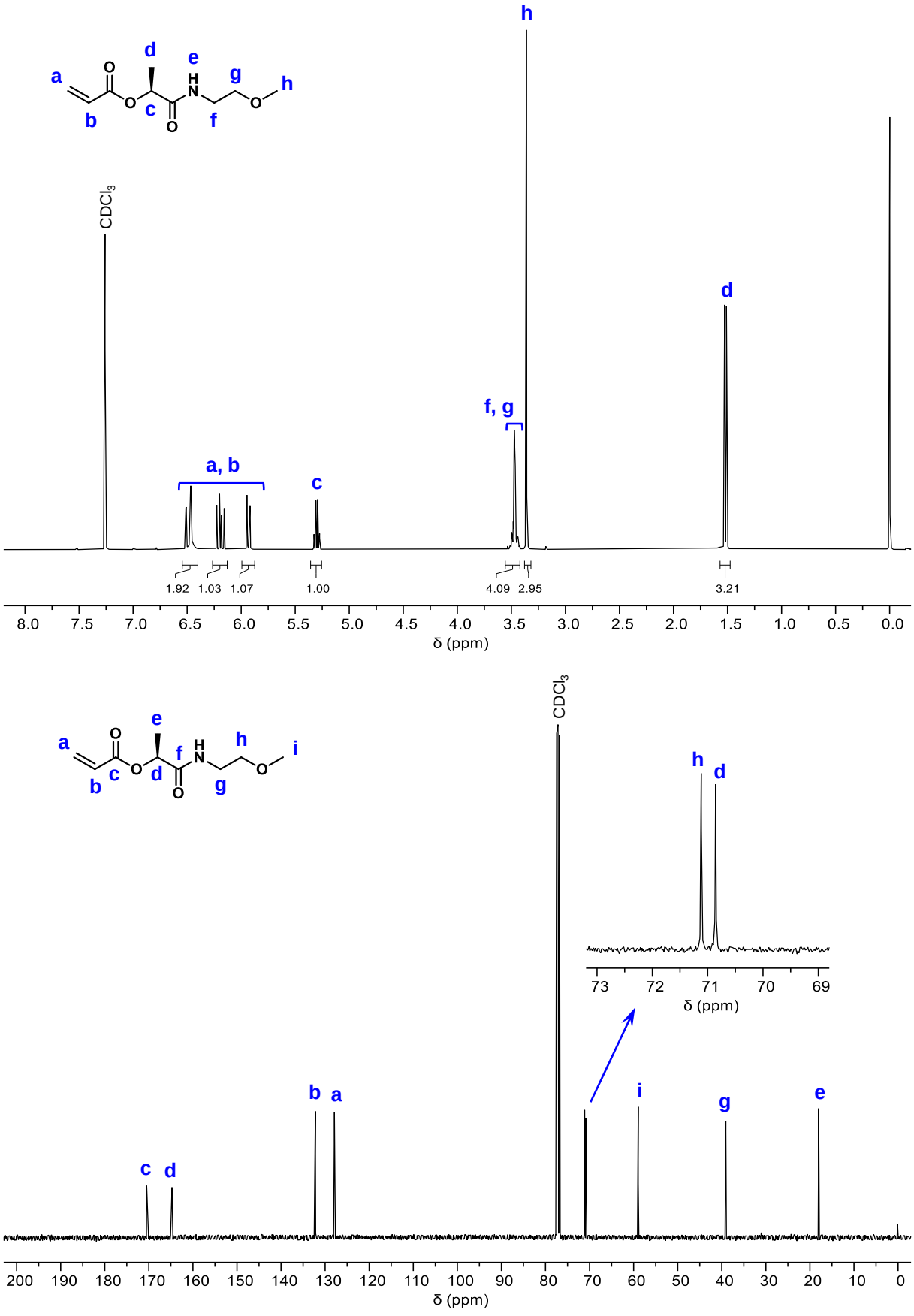

Figure S12. ^{1}H (top) and ^{13}C (bottom) NMR spectra of LAA5 in $CDCl_3$.

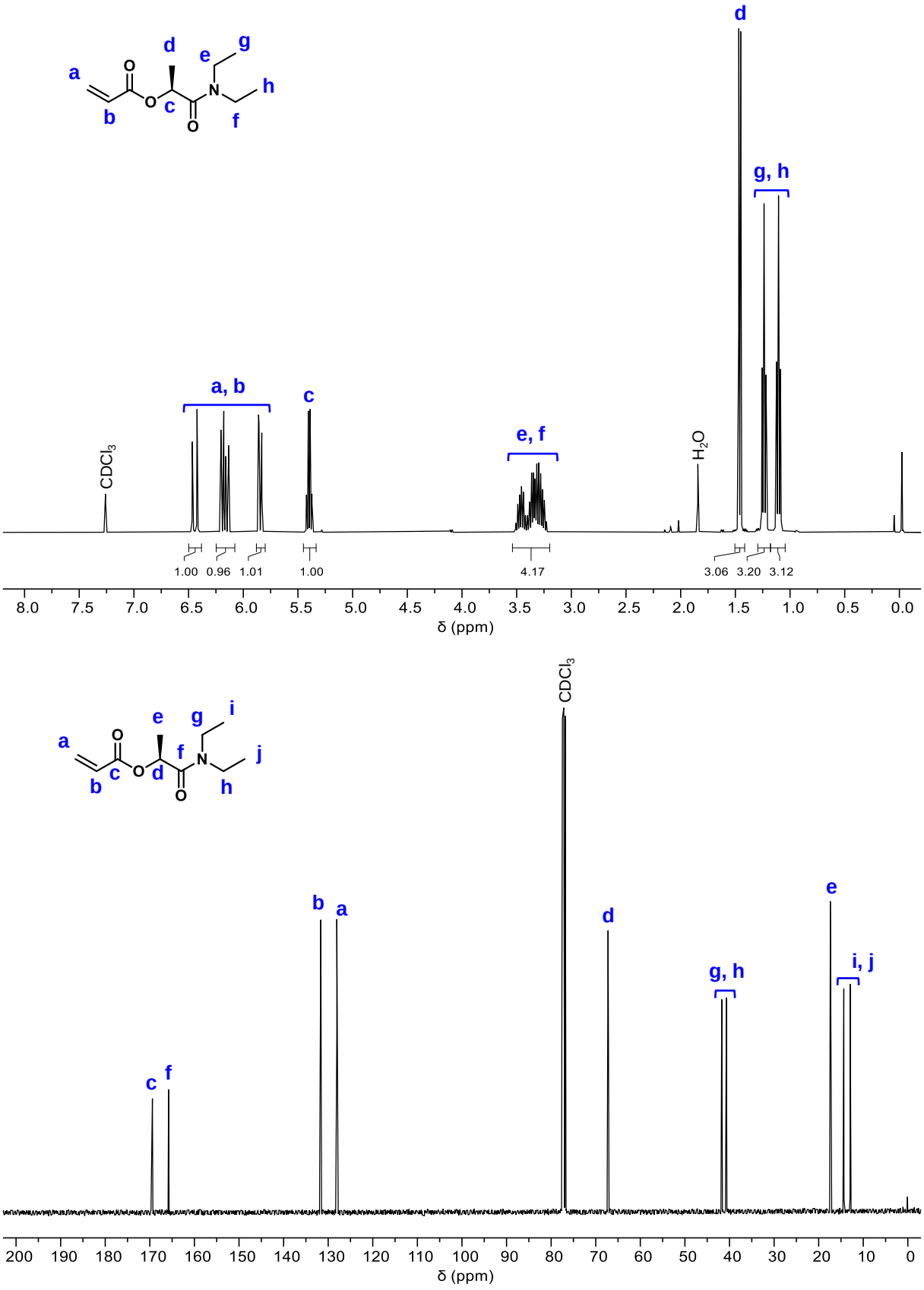

Figure S13. ^{1}H (top) and ^{13}C (bottom) NMR spectra of LAA6 in $CDCl_3$.

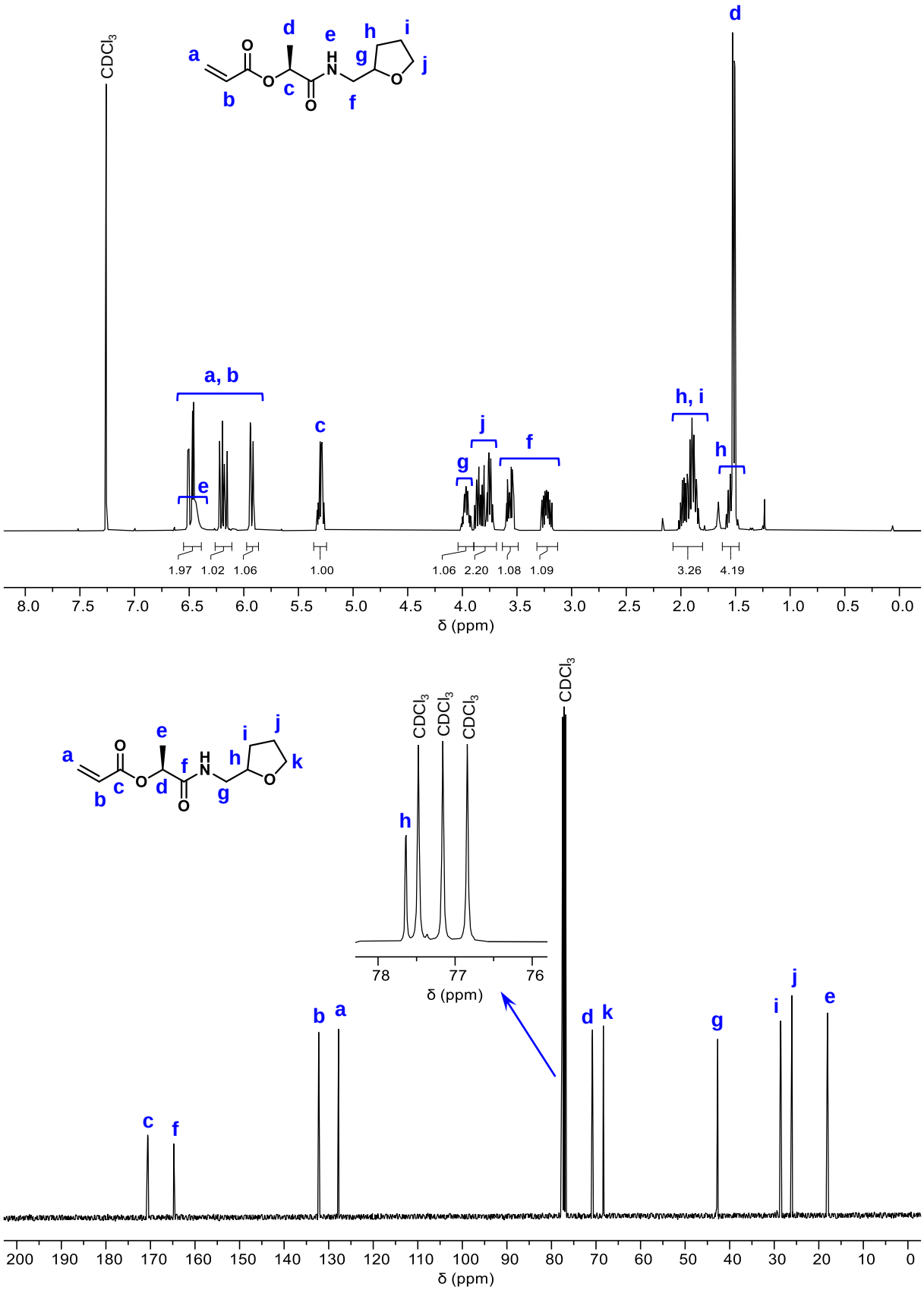

Figure S14. ^{1}H (top) and ^{13}C (bottom) NMR spectra of LAA7 in $CDCl_3$.

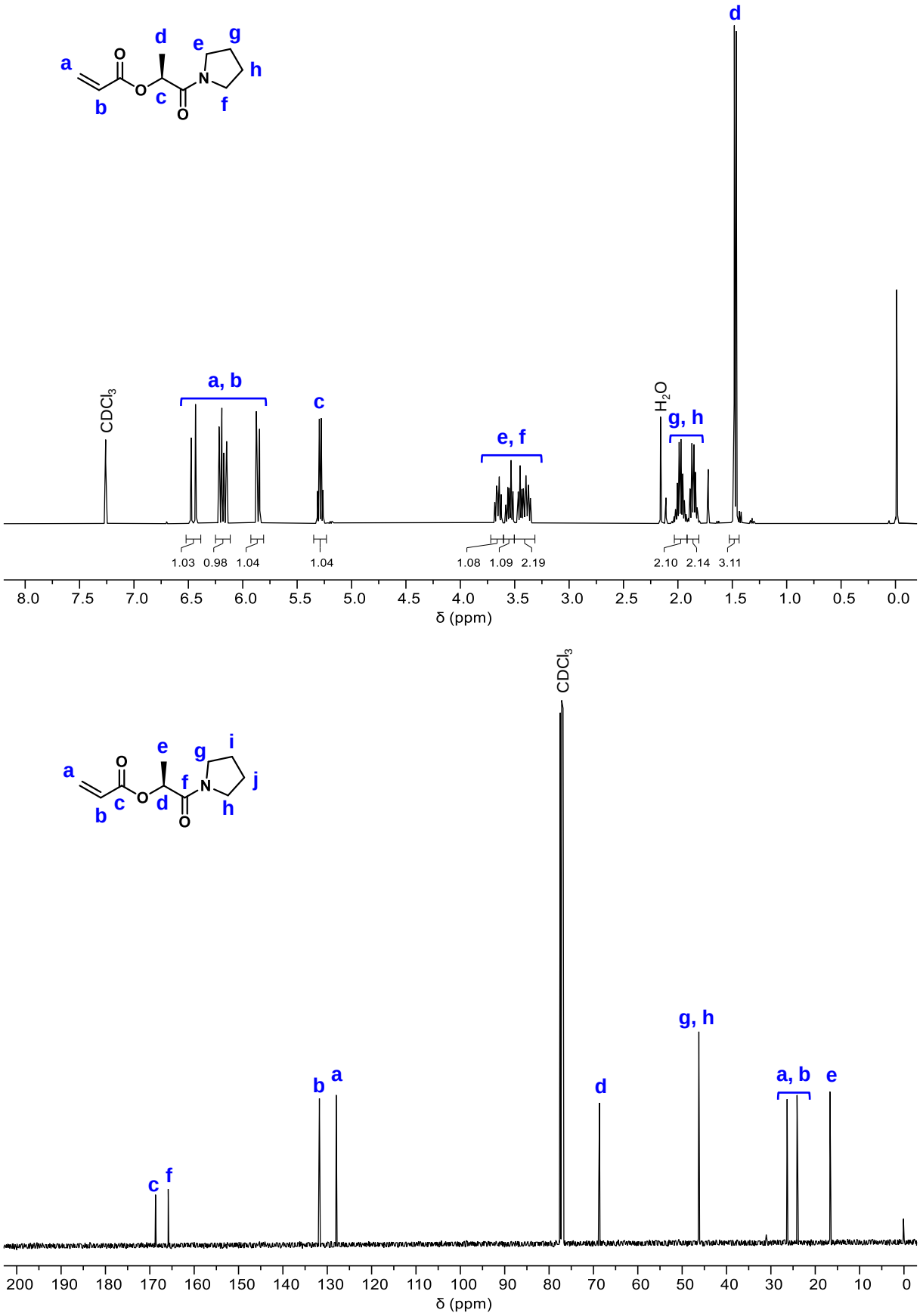

Figure S15. ^{1}H (top) and ^{13}C (bottom) NMR spectra of LAA8 in $CDCl_3$.

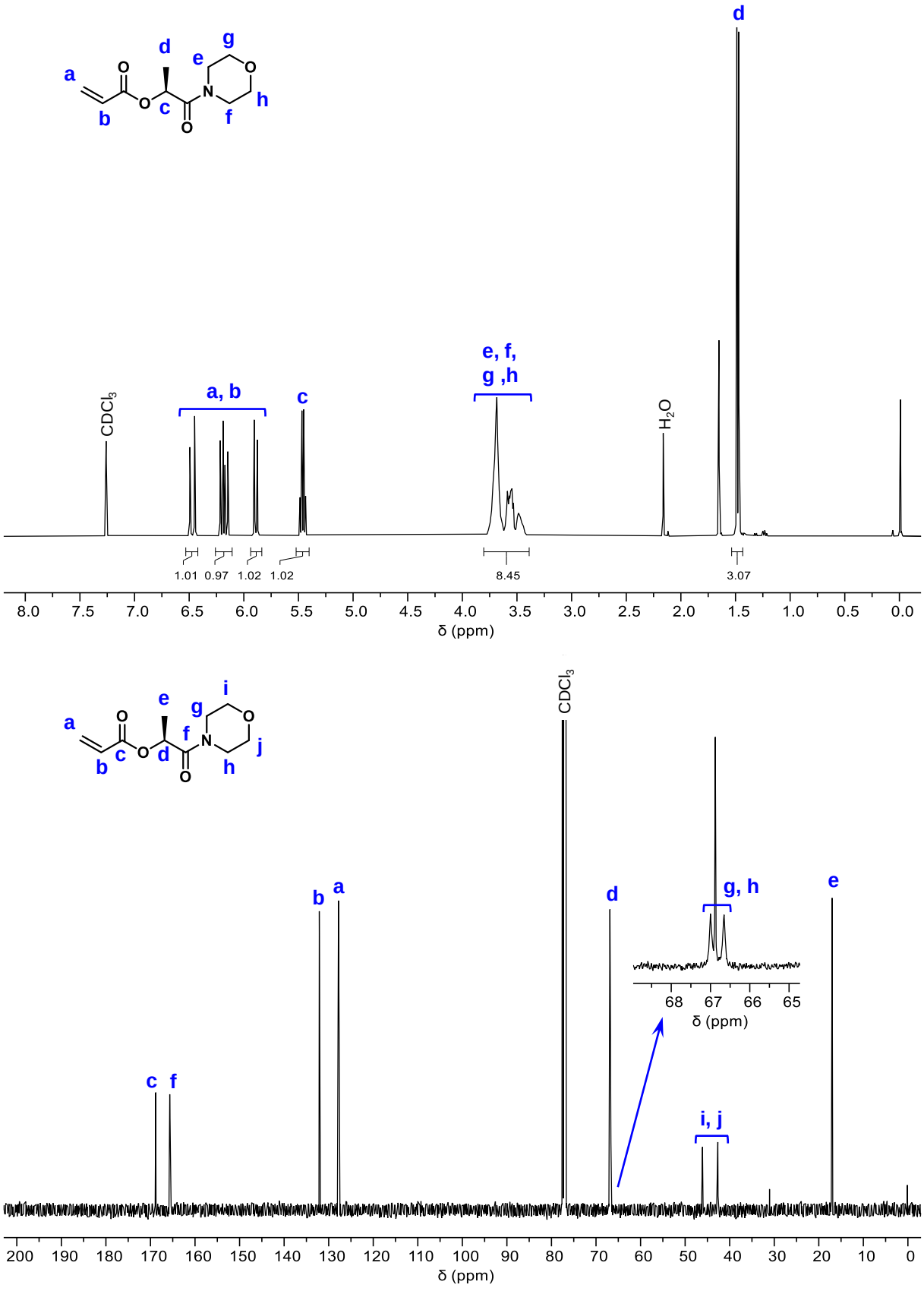

Figure S16. ^{1}H (top) and ^{13}C (bottom) NMR spectra of LAA9 in $CDCl_3$.

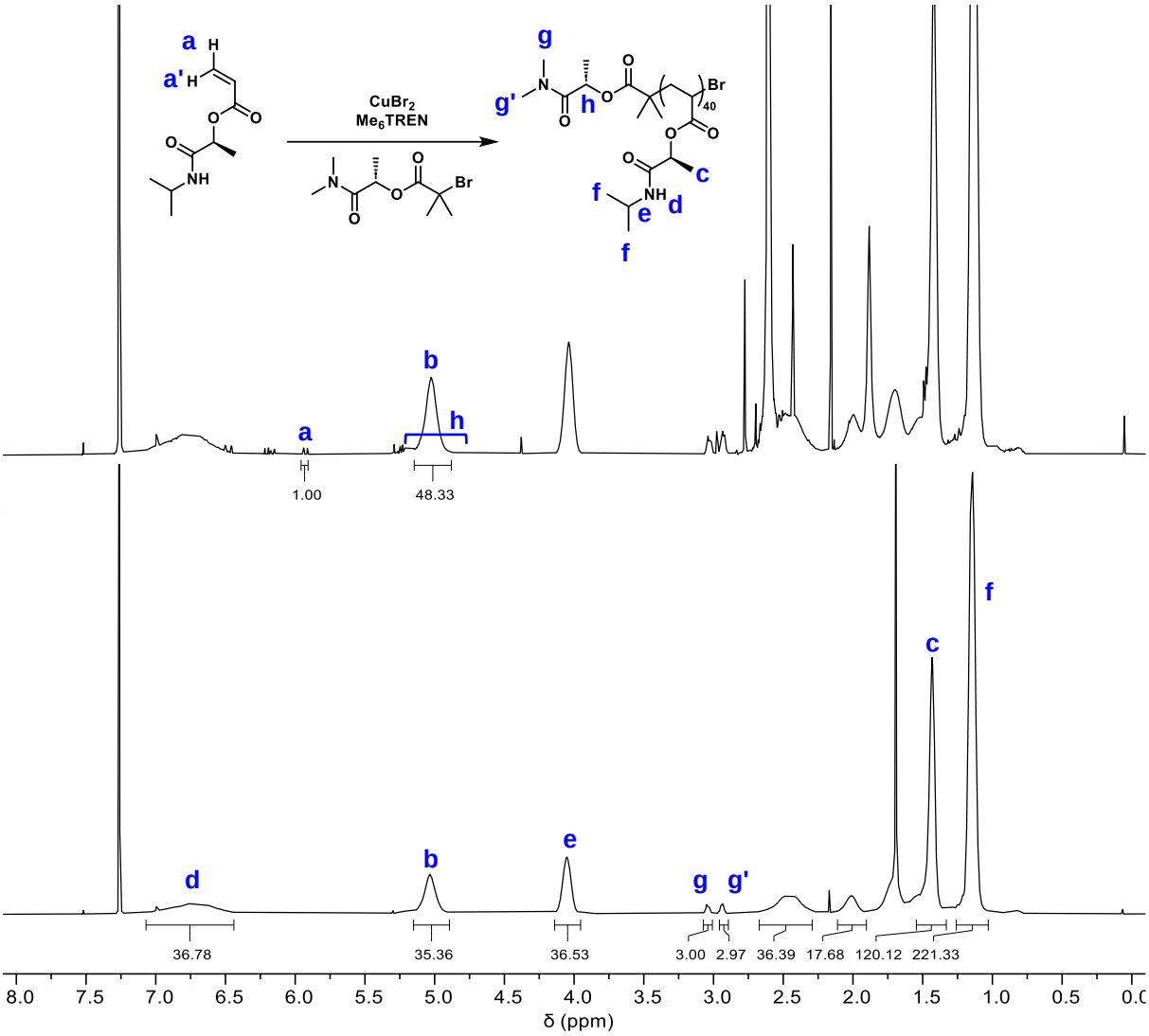

Figure S17. ^{1}H NMR spectra of homopolymerization of LAA4 by Cu(II)Br$_2$/Me$_6$TREN-mediated photopolymerization after 2.5 h of reaction time (top) and after dialysis (bottom).

Equations used for calculation of monomer conversion and molecular weight of PLAA4 by ^{1}H NMR (See Figure S17 for proton assignation)

$$Conv.(\%) = \frac{H^b - H^h}{(H^b - H^h) + H^a} \times 100 \qquad \text{(Equation S1)}$$

$$M^{NMR} = \frac{3(H^b - H^h)}{H^g} M_{LAA4} + M_{DMLBr} \qquad where\ H^h = \frac{H^g}{3} \qquad \text{(Equation S2)}$$

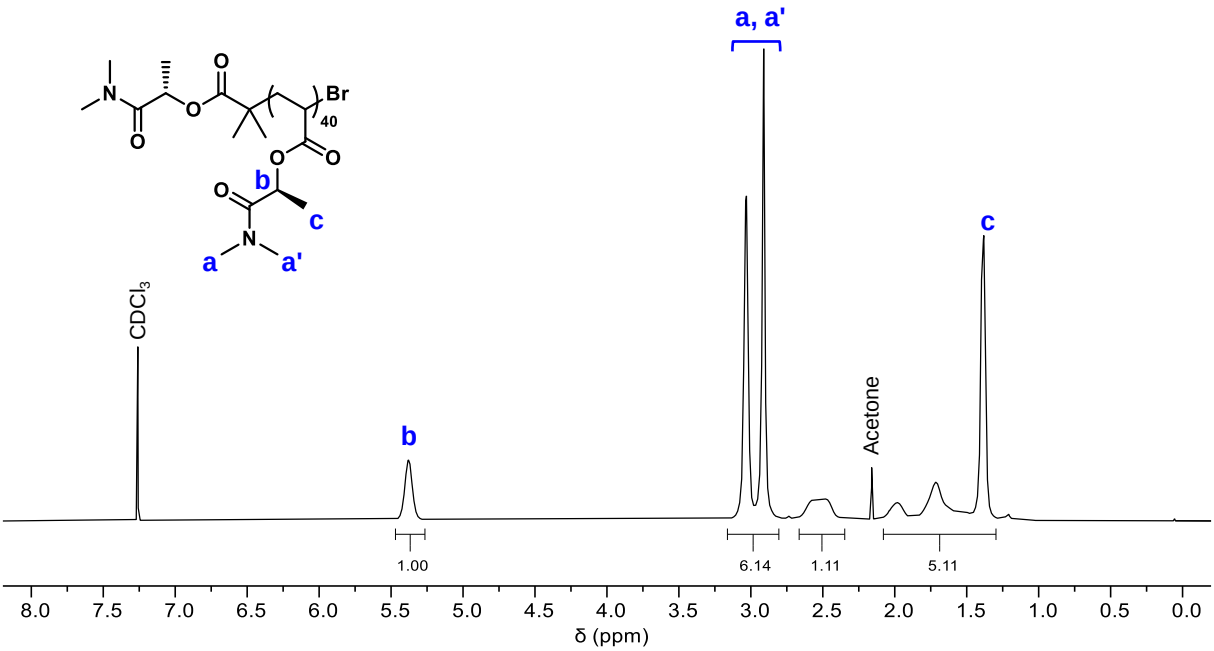

Figure S18. ^{1}H NMR spectra of PLAA0 in $CDCl_3$.

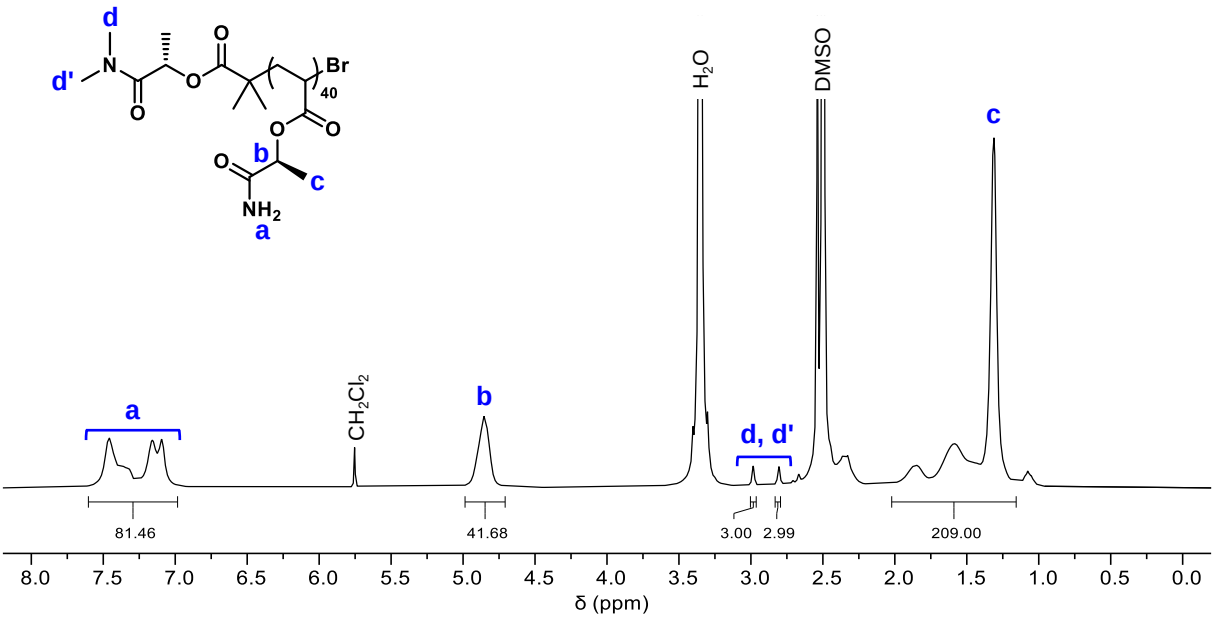

Figure S19. ^{1}H NMR spectra of PLAA1 in $CDCl_3$.

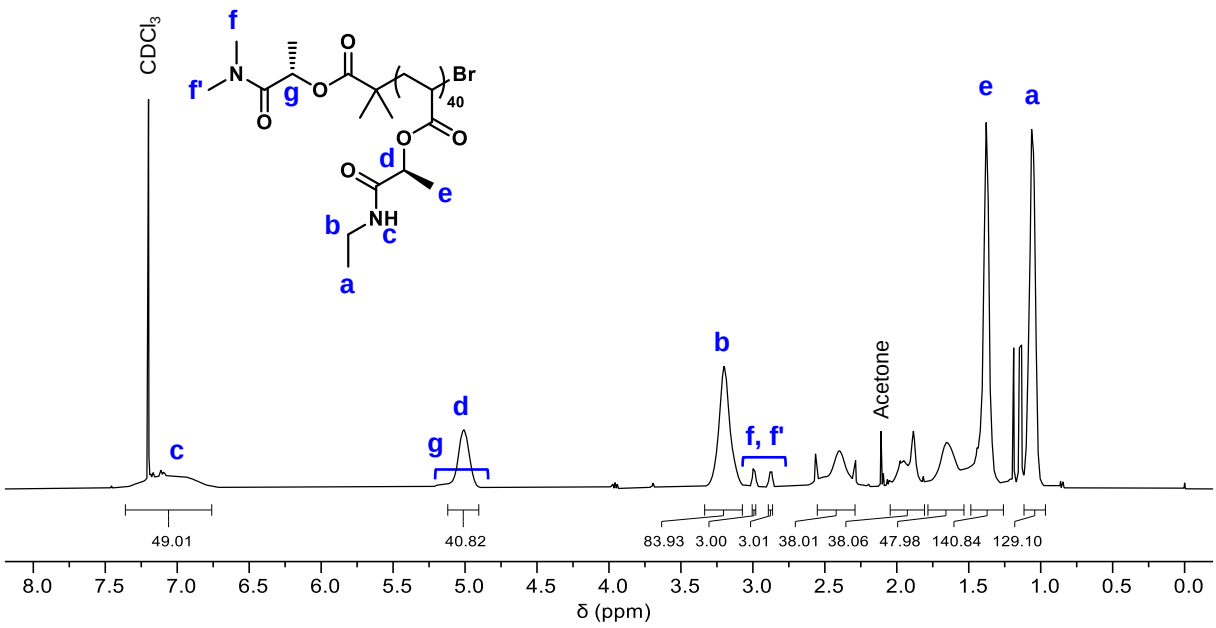

Figure S20. ^{1}H NMR spectra of PLAA2 in $CDCl_3$.

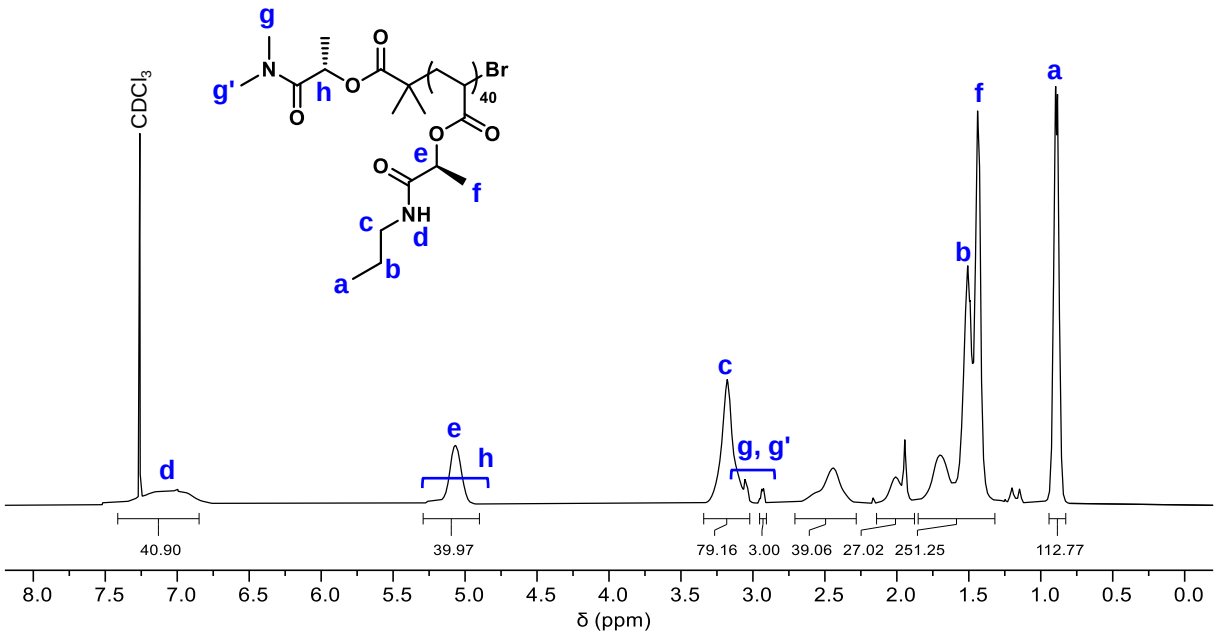

Figure S21. ^{1}H NMR spectra of PLAA3 in $CDCl_3$.

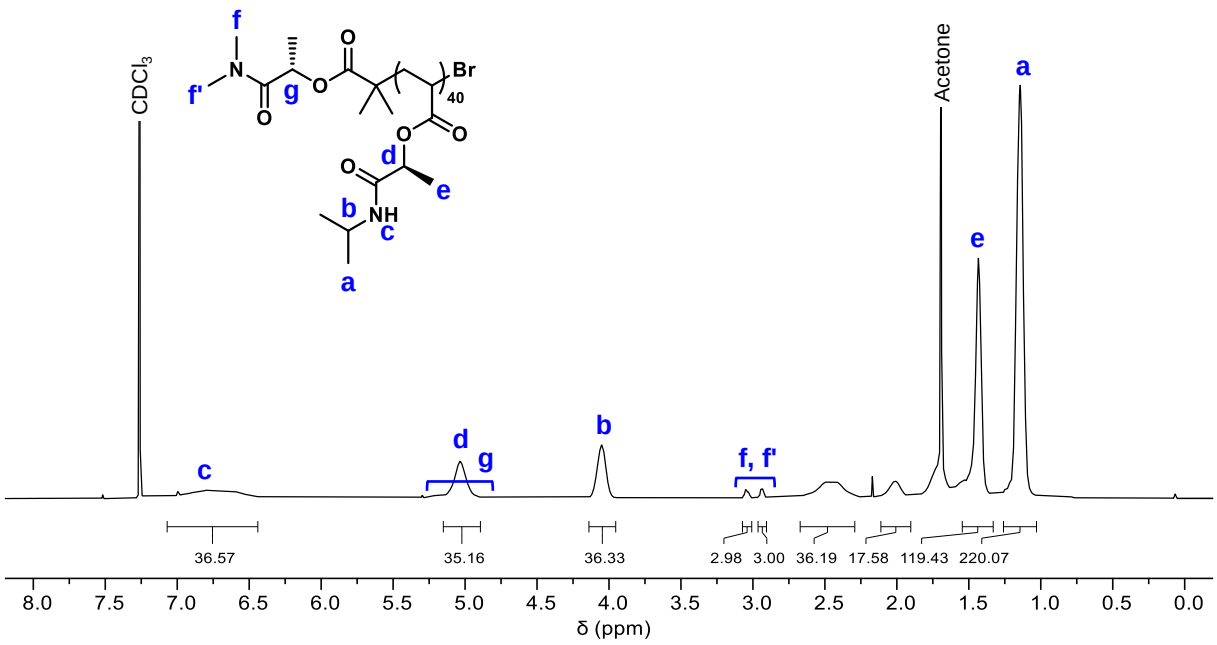

Figure S22. ^{1}H NMR spectra of PLAA4 in $CDCl_3$.

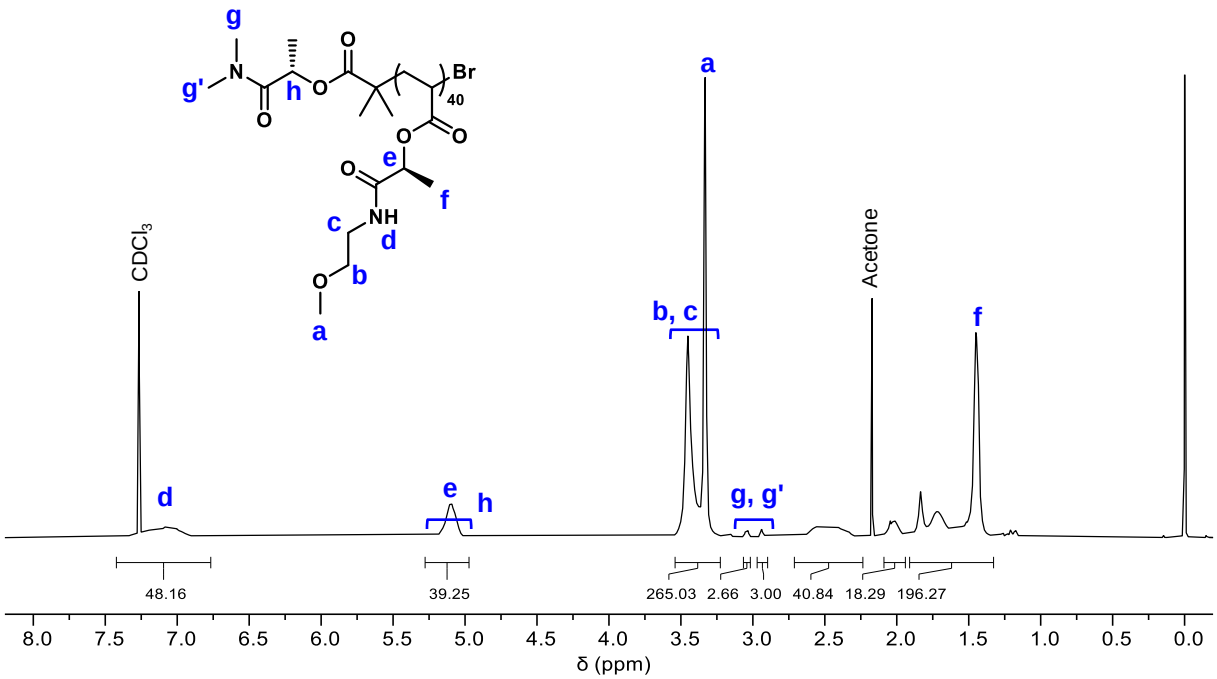

Figure S23. ^{1}H NMR spectra of PLAA5 in $CDCl_3$.

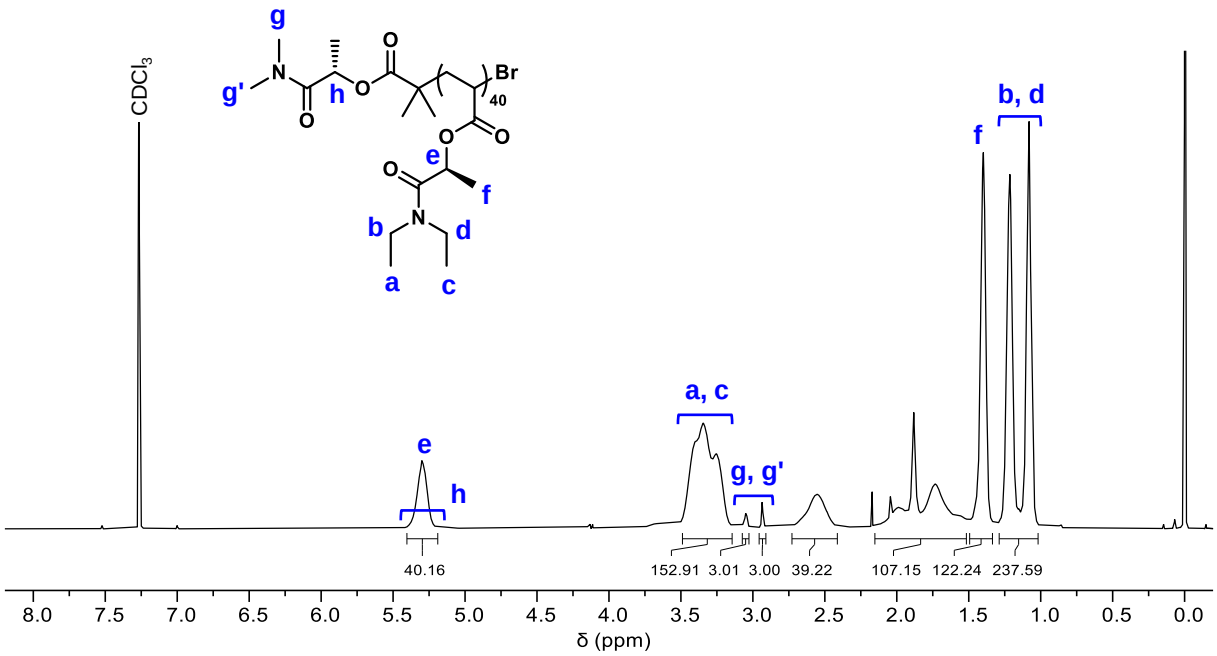

Figure S24. ^{1}H NMR spectra of PLAA6 in $CDCl_3$.

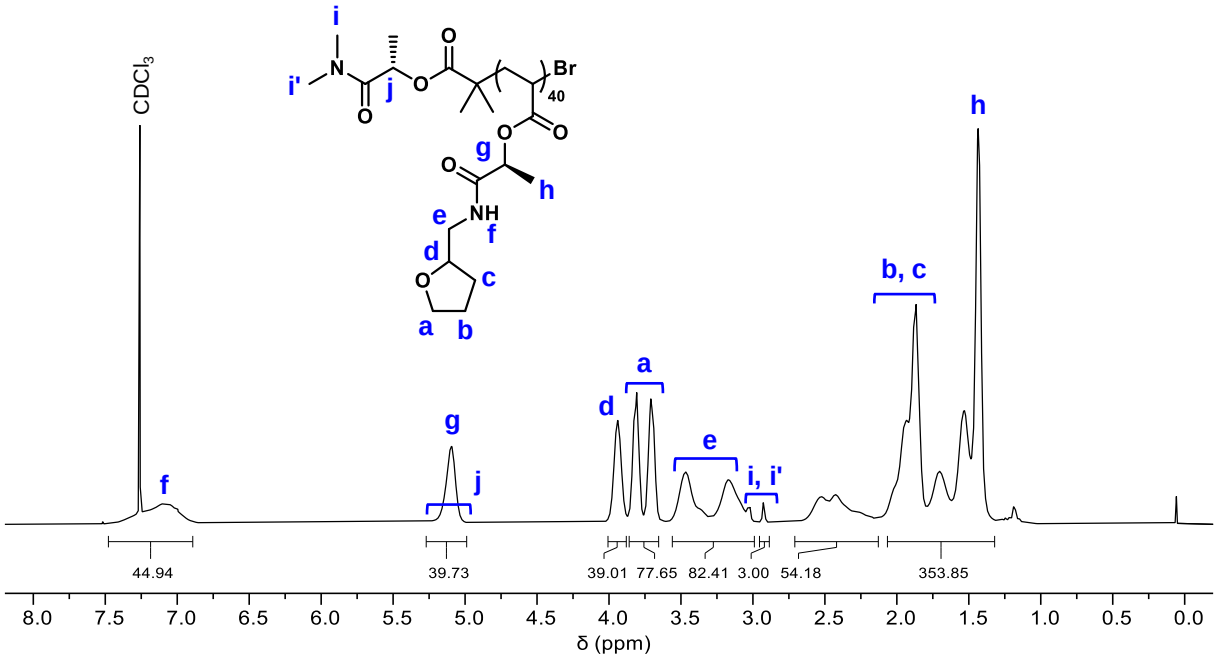

Figure S25. ^{1}H NMR spectra of PLAA7 in $CDCl_3$.

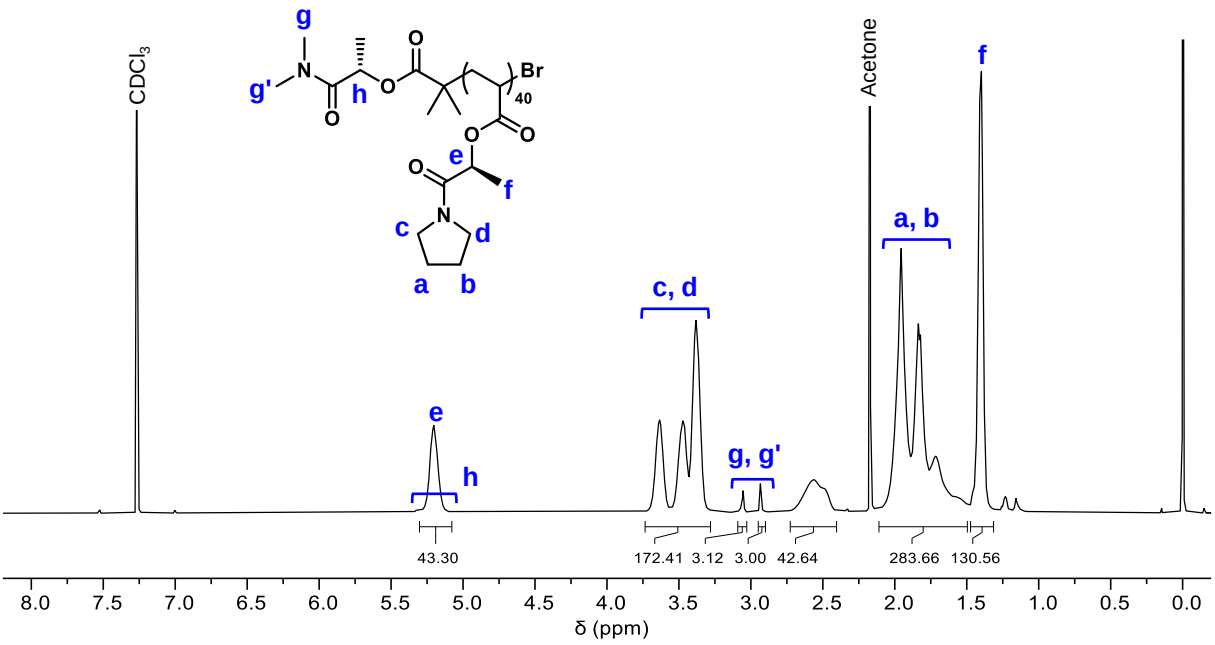

Figure S26. ^{1}H NMR spectra of PLAA8 in $CDCl_3$.

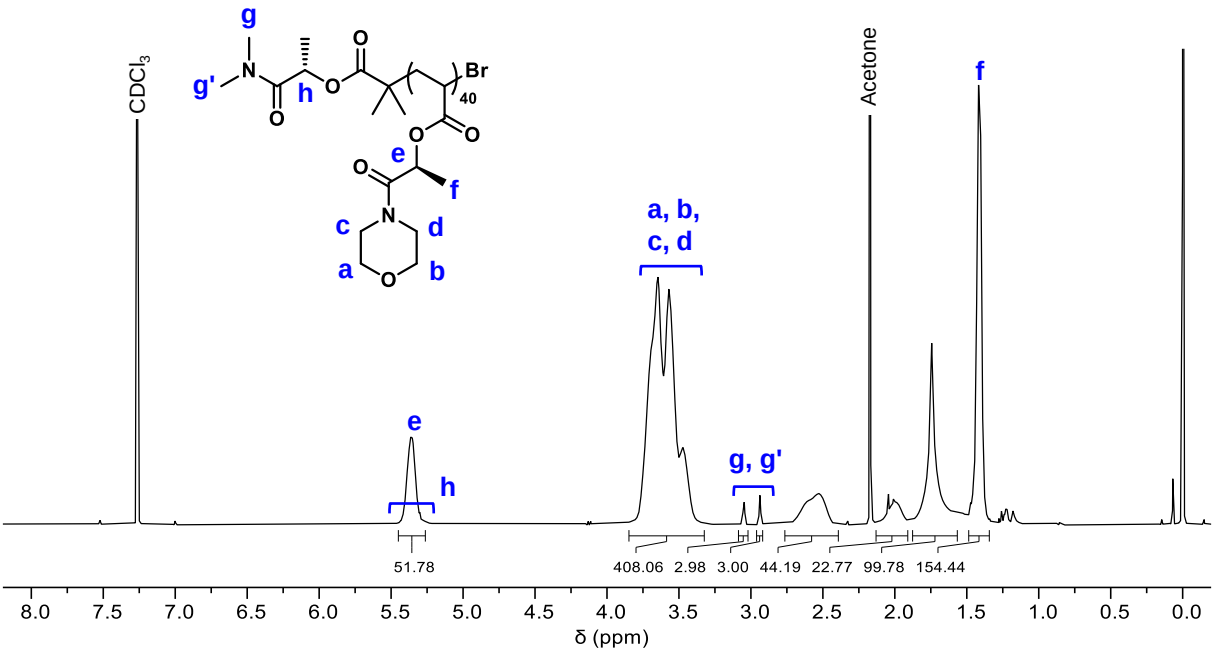

Figure S27. ^{1}H NMR spectra of PLAA9 in $CDCl_3$.

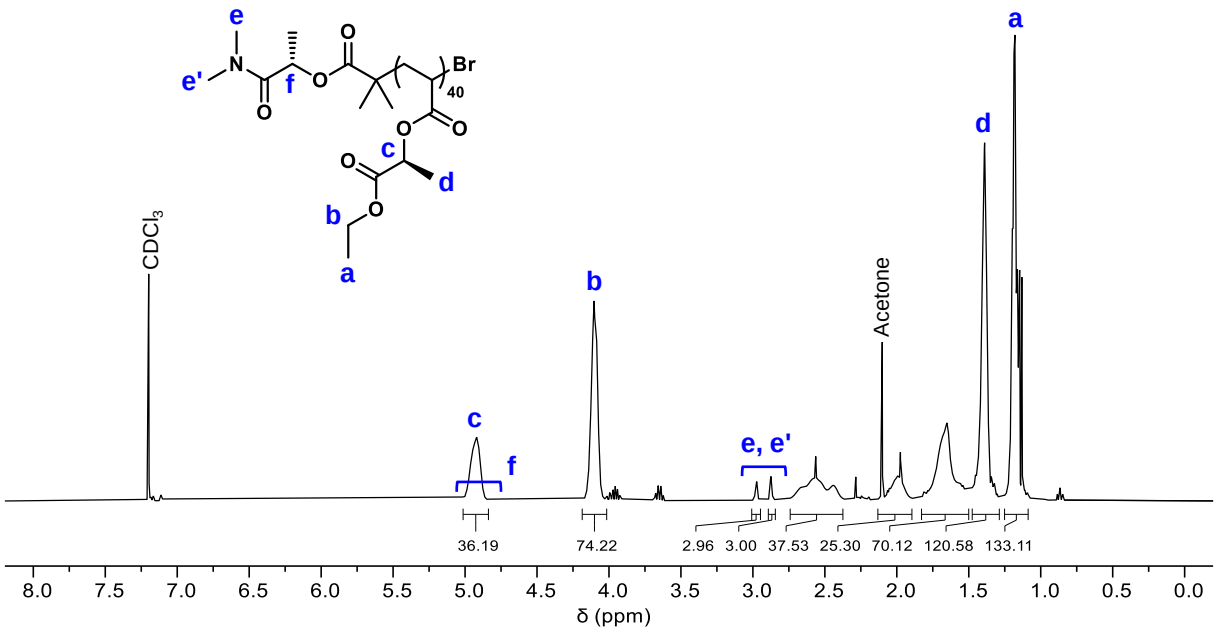

Figure S28. ^{1}H NMR spectra of PELA in $CDCl_3$.

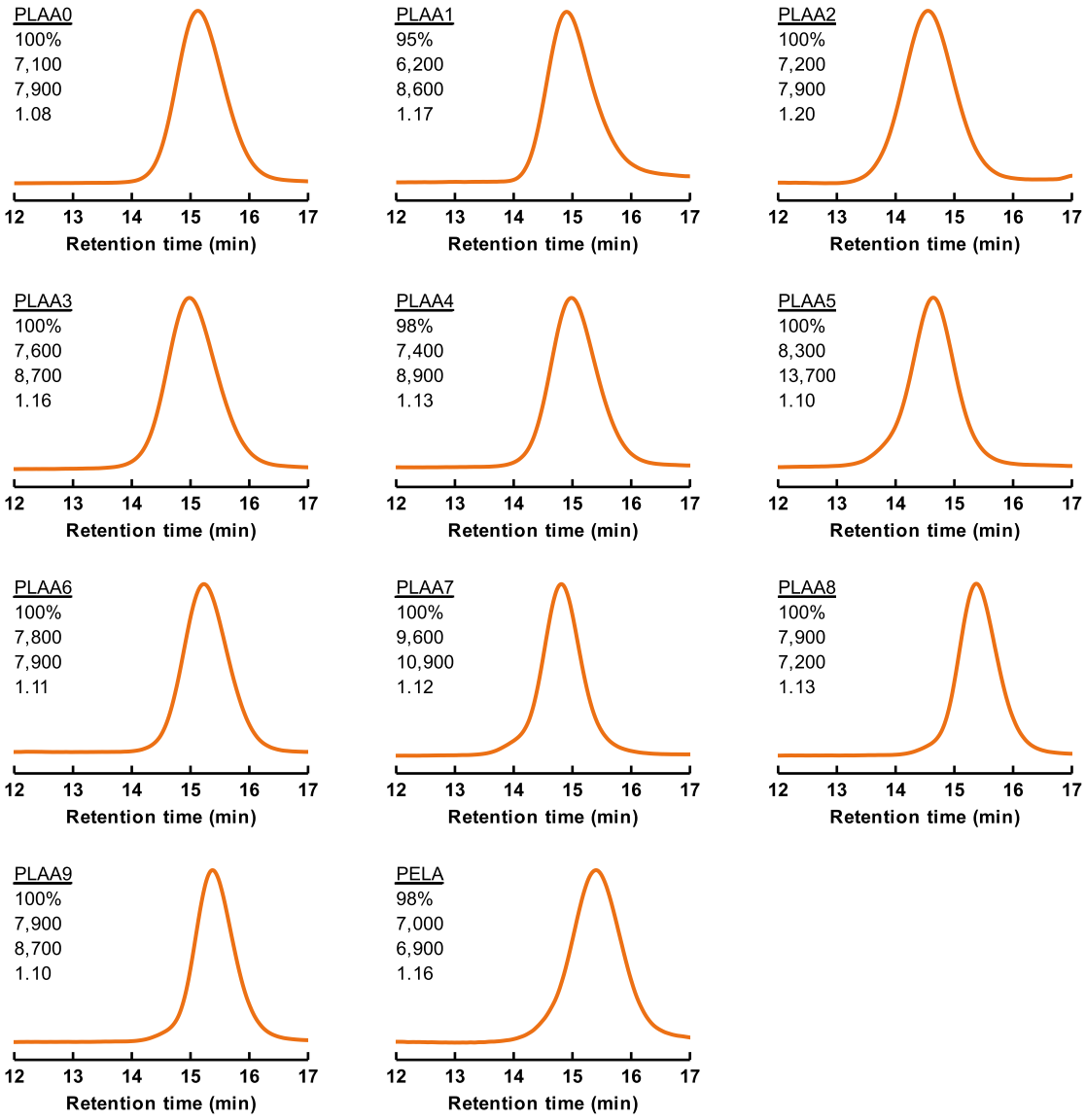

Figure S29. SEC traces of PLAAs after dialysis against acetone. Numbers shown together with SEC traces correspond to monomer conversion, M^{th}, $M_{\mathrm{n}}^{\mathrm{SEC}}$ and $Đ$, respectively, from the top to the bottom.

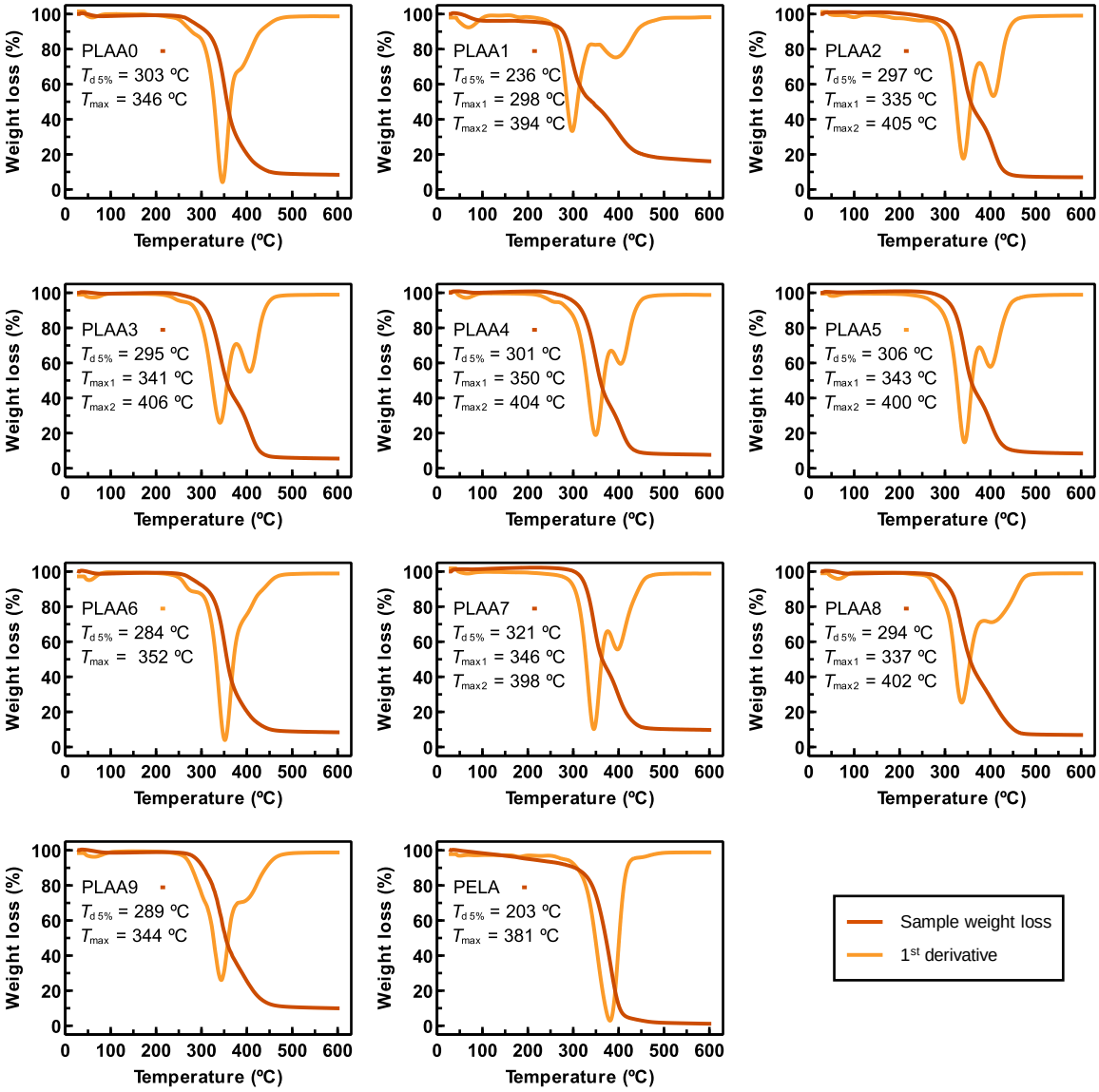

Figure S30. TGA and DTGA analysis of PLAA0–9 and PELA.

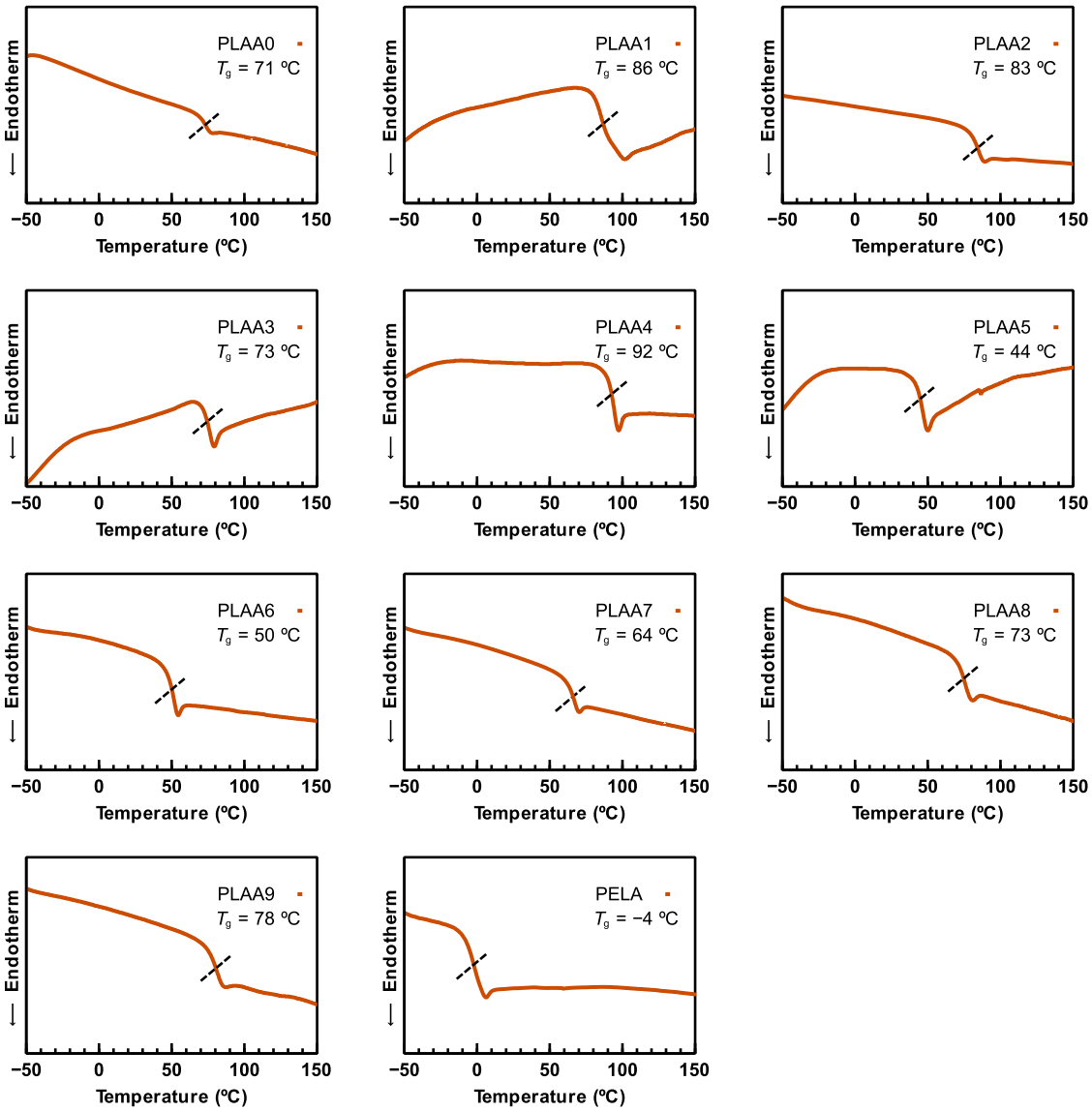

Figure S31. DSC analysis of PLAA0–9 and PELA.

Table S1. Cu(II)Br$_2$/Me$_6$TREN-mediated photopolymerization of LAA5 and LAA7 using DMLBr as the initiator.[a]

Ref.	Feed ratio (LAA5:LAA7, %)	Conv.[b] (%)	M^{th} [c]	M^{NMR} [d]	M_n^{SEC} [e]	$Đ$ [e]	LAA5: LAA7 [d] (%)	T_g [f] (ºC)	T_{cp} [g] (ºC)
SCP1	30:70	96	8,600	8,300	9,100	1.13	32:68	53	29
SCP2	40:60	100	9,100	8,500	10,000	1.14	40:60	52	33
SCP3	50:50	100	8,900	8,900	10,200	1.16	50:50	50	36
SCP4	60:40	100	8,900	8,700	11,800	1.14	57:43	50	39
SCP5	70:30	100	8,700	8,600	11,400	1.15	70:30	49	45

[a] Reaction conditions ([LAA5]$_0$ + [LAA7]$_0$) : [DMLBr]$_0$: [Cu(I)Br]$_0$: [Me$_6$TREN]$_0$ = 40 : 1 : 0.8 : 0.6, reaction time 2.5 h. [b] Determined by ^{1}H NMR. [c] M^{th} = (201.22 × LAA5 ratio + 227.26 × LAA7 ratio) × ([LAA5]$_0$ + [LAA7]$_0$) / [DMLBr]$_0$ × conv. + 266.14. [d] Determined by ^{1}H NMR after dialysis using Equation S5. [e] Determined by SEC using PMMA standards. [f] Determined by DSC at 20 °C·min^{-1}. [g] Determined by UV/Vis spectroscopy (5 mg·mL^{-1}).

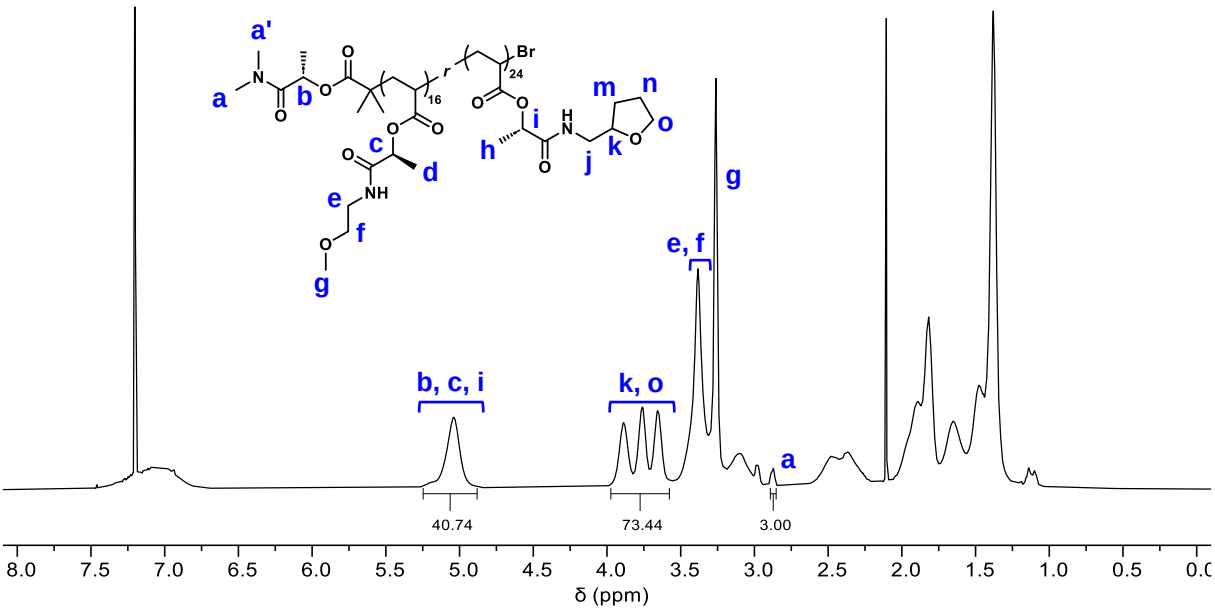

Figure S32. ^{1}H NMR spectra of SCP2 in CDCl$_3$.

Equations used for calculation of comonomer composition and molecular weight of SCP1–5 by ^{1}H NMR (see Figure S32 for proton assignation)

$$DP_{LAA7} = \frac{H^k + H^o}{H^a} \quad \text{(Equation S3)}$$

$$DP_{LAA5} = \left(H^b + H^c + H^i\right) - DP_{LAA7} - \frac{H^a}{3} \quad \text{(Equation S4)}$$

$$M^{NMR} = DP_{LAA5} \cdot M_{LAA5} + DP_{LAA7} \cdot M_{LAA7} + M_{DMLBr} \quad \text{(Equation S5)}$$

Table S2. Ecotoxicology results of the test compounds for all tested organisms.

Compound	Reference	*A. fischeri* (EC_{50}, mg·L^{-1})	*S. polyrhiza* (EC_{50}, mg·L^{-1})	*T. Platyrus* (EC_{50}, mg·L^{-1})
Monomers	LAA0	>8,000	17.49	5.5
			16.03	6.2
			17.36	5.3
	LAA5	>8,000	32.34	5.7
			29.85	7.6
			35.91	6.2
	LAA7	490	17.03	5.7
		385	16.49	5.4
		400	13.82	5.1
	LAA9	>8,000	38.62	5.5
			43.52	7.2
			35.48	5.7
Polymers	PLAA0	>20,000	>1,000	>1,000
	PLAA5	14,860	566	308
		14,853	534	479
		14,200	496	394
	PLAA7	6,435	288	223
		6,975	361	301
		6,620	325	265
	PLAA9	3,850	488	249
		3,925	335	297
		3,970	497	211

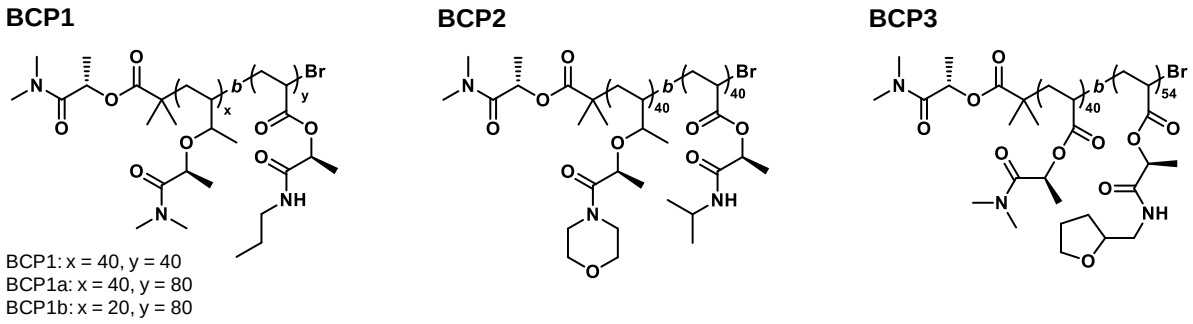

Figure S33. Chemical structures of BCP1, BCP2 and BCP3.

Table S3 Controlled diblock polymerization of various LAA monomers by $Cu(II)Br_2$ /Me_6TREN-mediated photopolymerization DMLBr as the initiator.[a]

Ref.	Monomer feed (B1:B2)	Block 1 (B1)			Block 2 (B2)					B1:B2 [f] (wt%)
		Conv.[b] (%)	M^{th} [c]	M_n^{SEC} [d]	Conv.[b] (%)	M^{th} [c]	M^{NMR} [e]	M_n^{SEC} [d]	$Đ$ [d]	
BCP1	$LAA0_{40}$:$LAA3_{40}$	99	7,300	7,400	96	14,500	14,500	15,600	1.16	47:53
BCP1a	$LAA0_{40}$:$LAA3_{80}$	99	7,300	7,100	96	21,700	21,400	24,400	1.18	29:71
BCP1b	$LAA0_{20}$:$LAA3_{80}$	99	3,700	4,000	96	18,700	17,900	23,800	1.12	17:83
BCP4	$LAA9_{40}$:$LAA4_{40}$	100	8,600	7,800	87	15,000	14,700	15,500	1.21	50:50
BCP5	$LAA0_{40}$:$LAA7_{54}$	98	7,000	7,500	95	18,600	20,000	18,200	1.20	41:59

[a] Reaction conditions: $[DMLBr]_0 : [CuBr_2]_0 : [Me_6TREN]_0 = 1 : 0.02 : 0.12$. [b] Determined by ^1H NMR after 2h for the first block (B1) and after 3h for the second block (B2). [c] $M_{B1}^{th} = M_{LAA,\,B1} \times ([LAA, B1]_0 / [DMLBr]_0) \times conv. + 266.14$ and $M_{B2}^{th} = M_{B1}^{th} + [M_{LAA,\,B2} \times ([LAA, B2]_0 / [DMLBr]_0) \times conv.]$. [d] Determined by SEC using PMMA standards. [e] Determined by ^1H NMR using Equation S8 (BCP1, BCP1a, BCP1b), Equation S11 (BCP2), and Equation S14 (BCP3). [f] Determined using the M_n^{SEC} of each block.

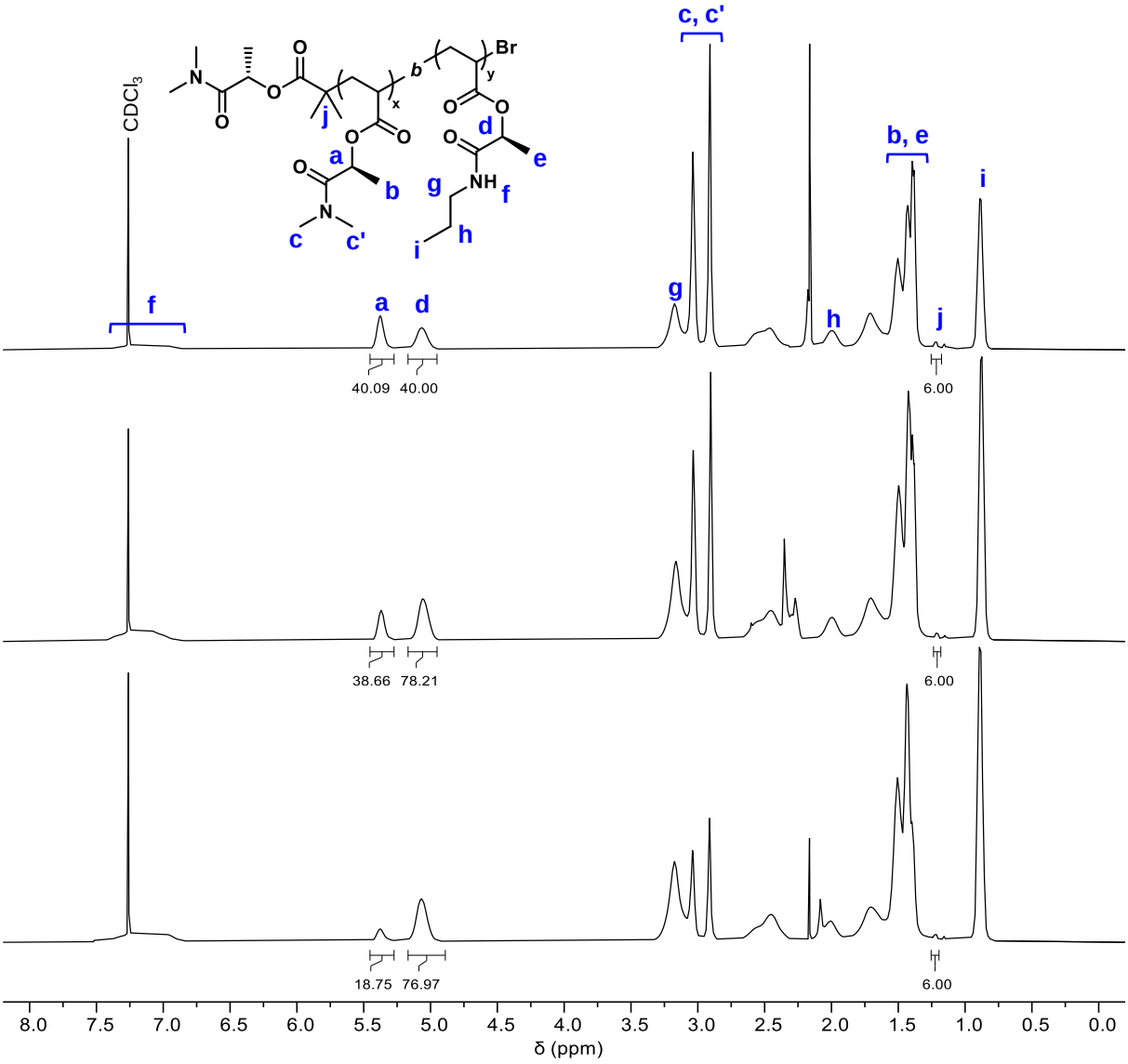

Figure S34. ^{1}H NMR spectra of BCP1 (top), BCP1a (middle) and BCP1b (bottom) in $CDCl_3$.

Equations used for the calculation of comonomer composition and molecular weight of BCP1, BCP1a and BCP1b by ^{1}H NMR (see Figure S34 for proton assignation)

$$DP_{LAA0} = \frac{6H^{a}}{H^{j}} \quad \text{(Equation S6)}$$

$$DP_{LAA3} = \frac{6H^{d}}{H^{j}} \quad \text{(Equation S7)}$$

$$M^{NMR} = DP_{LAA0} \cdot M_{LAA0} + DP_{LAA3} \cdot M_{LAA3} + M_{DMLBr} \quad \text{(Equation S8)}$$

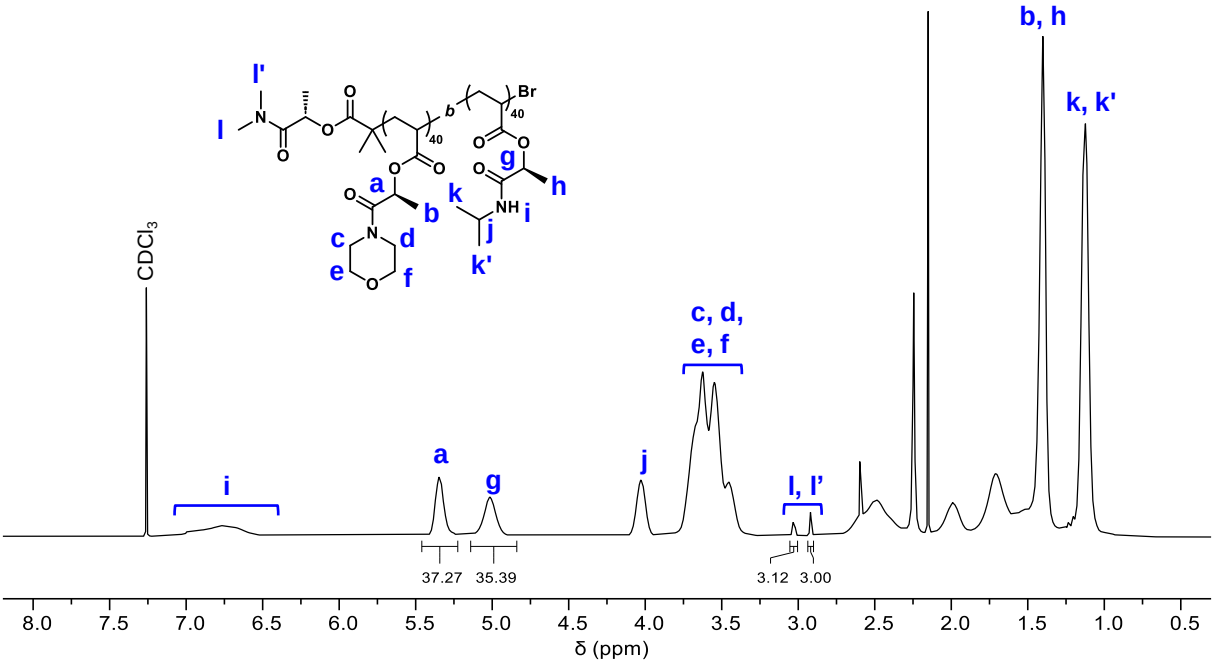

Figure S35. ^{1}H NMR spectra of BCP2 in $CDCl_3$.

Equations used for the calculation of comonomer composition and molecular weight of BCP2 by ^{1}H NMR (see Figure S35 for proton assignation)

$$DP_{LAA8} = \frac{3H^{a}}{H^{l}} \quad \text{(Equation S9)}$$

$$DP_{LAA4} = \frac{3H^{g}}{H^{l}} \quad \text{(Equation S10)}$$

$$M^{NMR} = DP_{LAA8} \cdot M_{LAA8} + DP_{LAA4} \cdot M_{LAA4} + M_{DMLBr} \quad \text{(Equation S11)}$$

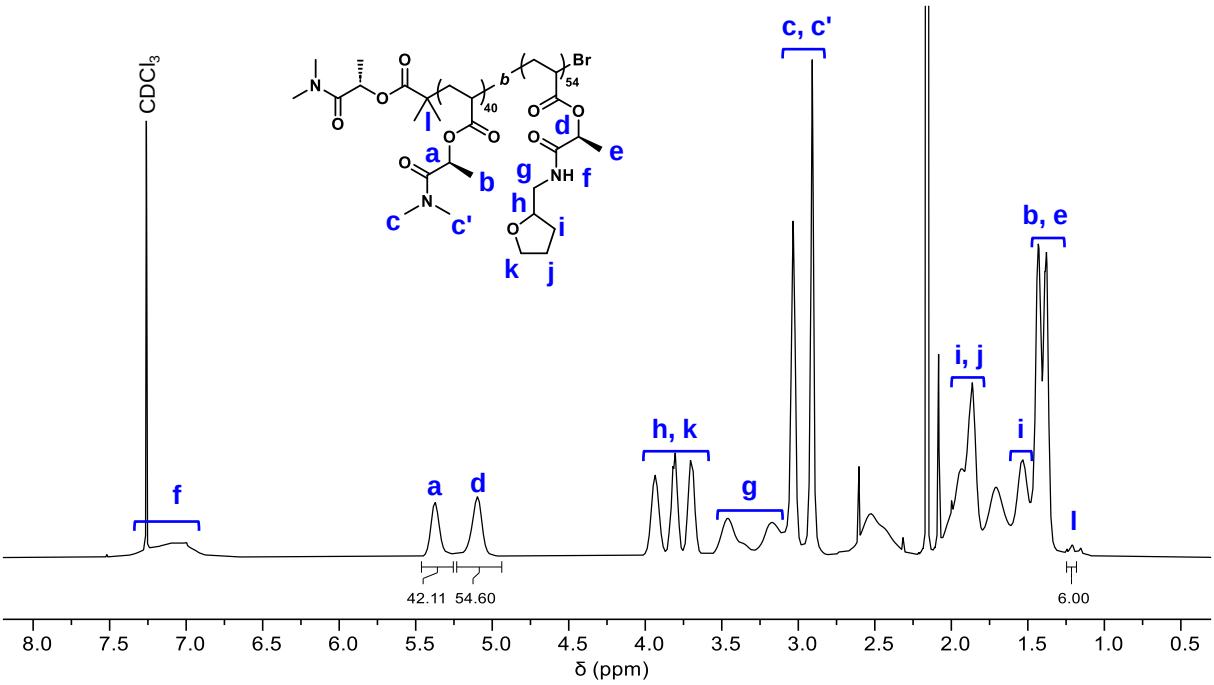

Figure S36. ^{1}H NMR spectra of BCP3 in $CDCl_3$.

Equations used for the calculation of comonomer composition and molecular weight of BCP2 by ^{1}H NMR (see Figure S36 for proton assignation)

$$DP_{LAA0} = \frac{6H^{a}}{H^{l}} \quad \text{(Equation S12)}$$

$$DP_{LAA7} = \frac{6H^{d}}{H^{l}} \quad \text{(Equation S13)}$$

$$M^{NMR} = DP_{LAA0} \cdot M_{LAA0} + DP_{LAA7} \cdot M_{LAA7} + M_{DMLBr} \quad \text{(Equation S14)}$$

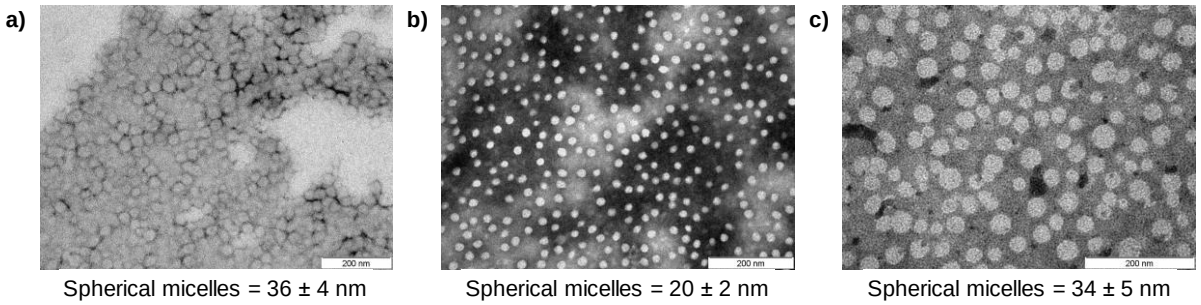

Figure S37. TEM images of self-assemble nanoparticles from (a) BCP1, (b) BCP2 and (c) BCP3.

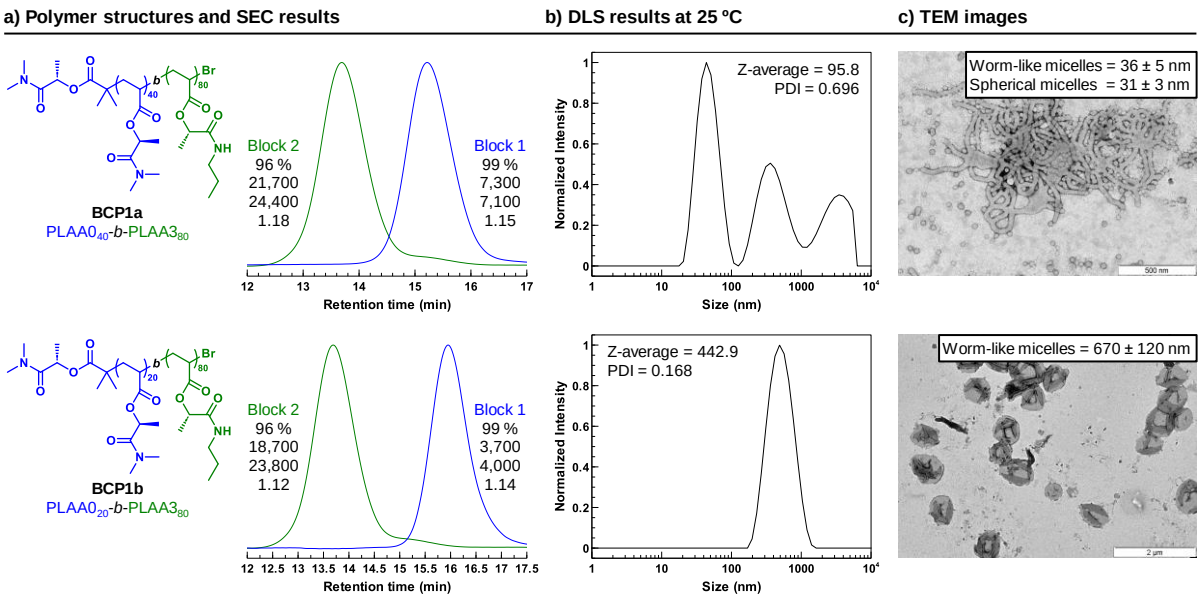

Figure S38. Characterization of the diblock copolymer BCP1a and BCP1b and the self-assembled nano particles. a) Chemical structures of the diblock copolymers and SEC traces. Numbers shown together with SEC traces correspond to monomer conversion, M^{th}, $M_{\mathrm{n}}^{\mathrm{SEC}}$ and $Đ$, respectively, from the top to the bottom. b) Size of diblock copolymer nanoparticles by DLS. c) TEM images of the diblock copolymer nanoparticles.

LAA0 and LAA3 were copolymerized at varying [LAA3]/[LAA0] molar ratios to produce two additional amphiphilic BCPs (BCP1a and BCP 1b) with higher molar ratio of hydrophobic block than BCP1 (Figure S34). Nanoparticles of these amphiphilic BCPs having LA0 bearing chains as hydrophilic block and LA3 as hydrophobic one were prepared *via* solvent-to-water method. Slow-injection of water droplets into BCP dissolved in THF ensures to obtain thermodynamically stable self-assembled structures. The morphology and size of the resulting nanoparticles were analyzed by TEM and DLS. Increasing the hydrophobic content of the copolymer in BCP1, BCP1a, and BCP1b led to the formation of self-assembled nanoparticles, with hydrodynamic diameters (determined by DLS) increasing from approximately 25 nm to 442 nm. TEM imaging clearly revealed morphological changes across different compositions. While BCP1 self-organized into clustered, irregular spherical micelles displaying an average diameter of 36 nm, BCP1a predominantly formed worm-like micelles, coexisting with a smaller fraction of spherical micelles. The width is around 36 nm. Further increase of molar ratio of hydrophobic block (for BCP1b) allowed fabricating vesicular structures composed of a bilayer of amphiphilic BCP with much potential in nanomedicine.